

Cite this: DOI: 10.1039/c1cs15103g

www.rsc.org/csr

CRITICAL REVIEW

Fabrication and application of inorganic hollow spheres

Jing Hu,^{ab} Min Chen,^a Xiaosheng Fang^a and Limin Wu^{*a}

Received 25th April 2011

DOI: 10.1039/c1cs15103g

Inorganic hollow spheres have attracted considerable interest due to their singular properties and wide range of potential applications. In this *critical review*, we provide a comprehensive overview of the preparation and applications of inorganic hollow spheres. We first discuss the syntheses of inorganic hollow spheres by use of polymers, inorganic nonmetals, metal-based hard templates, small-molecule emulsion, surfactant micelle-based soft-templates, and the template-free approach. For each method, a critical comment is given based on our knowledge and related research experience. We go on to discuss some important applications of inorganic hollow spheres in 0D, 2D, and 3D arrays. We conclude this review with some perspectives on the future research and development of inorganic hollow spheres (235 references).

1. Introduction

Monodisperse hollow spheres have attracted considerable interest in the past few decades due to their well-defined morphology, uniform size, low density, large surface area, and wide range of potential applications. For instance, the large fraction of void space in hollow structures has been used to load and control releasing systems for special materials, such as drugs, genes, peptides, spiceries, and biological molecules.¹ They can also be used to modulate refractive index,

lower density, increase the active area for catalysis and adsorption, improve particles' ability to withstand cyclic changes in volume, and expand the array of imaging markers suitable for early detection of cancer.^{2,3}

Inorganic hollow spheres have special optical, optoelectronic, magnetic, electrical, thermal, electrochemical, photoelectrochemical, mechanical, and catalytic properties, suggesting that they comprise a more common, more diverse, and probably richer class of materials than organic hollow spheres.⁴ Beginning with the pioneering work carried out by Kowalski and colleagues at Rohm and Haas,^{5,6} a variety of chemical and physicochemical strategies, including heterophase polymerization/combined with a sol-gel process,⁷ emulsion/interfacial polymerization methods,^{8–10} self-assembly techniques,^{11,12} and surface living polymerization process^{13–15} have been

^a Department of Materials Science and the Key Laboratory of Molecular Engineering of Polymers of MOE, Fudan University, Shanghai 200433, P. R. China. E-mail: lmw@fudan.edu.cn

^b School of Perfume and Aroma Technology, Shanghai Institute of Technology, Shanghai 200235, China



Jing Hu

Jing Hu received her PhD degree from Shaanxi University of Science and Technology in July, 2009. Then, she joined the School of Perfume and Aroma Technology of Shanghai Institute of Technology as a lecturer in perfume and aroma technology. In 2010, she was awarded "Shanghai Chenguang Scholar" by Shanghai municipality. Her current research interests include preparation and assembly of nanocapsules, function mechanism of sustained fragrance and propagation fibers.



Min Chen

Min Chen received her PhD degree from Fudan University under the supervision of Professor Limin Wu in 2006. Her dissertation was chosen as one of the "Top 100 National Excellent Doctoral Dissertations" in 2008. Just after finishing the doctorate work, she joined the Department of Materials Science, Fudan University, and was successively awarded "Shanghai Chenguang Scholar" and "Rising Star" by Shanghai municipality. She is currently an Associate Professor. Her research interests include the synthesis, characterization, assembly and properties of novel organic-inorganic hybrid nanostructured materials and inorganic hollow spheres.

employed to prepare inorganic hollow spheres. In particular, the template method is the most common. In this method, at least two steps are usually indispensable. First, the templates must be modified to give them the ability to coax inorganic precursors (salts or alkoxides) onto the surface of the template core. Then, after the inorganic shell is decorated outside the scaffold, the templates must be eliminated in some way, leaving behind a hollow shell. Generally, templates can be divided into hard and soft templates. When hard templates (*e.g.*, SiO_2 ,^{16–18} C spheres,¹⁹ polymers,^{20–24} metal particles²⁵) are employed, the structure of the hollow product is similar to that of the template, with a well-defined and monodisperse morphology. However, the removal of the templates by either thermal (sintering) or chemical (etching) means is very complicated and energy-consuming. As for soft templates (bacteria,^{26,27} droplets,²⁸ vesicles^{29,30} and more), although it is relatively easier to remove the templates, the morphology and monodispersity of the as-prepared hollow products are usually poor due to the deformability of the soft template. Although the drawbacks in these template strategies seem to be inherent and insurmountable, some novel techniques that seem to overcome them, such as sacrificial templates, modified soft templates, *etc.*, are emerging. Another important development in the preparation of inorganic hollow spheres is called the template-free method, such as the Ostwald ripening process, which not only combines the advantages of hard- and soft-template methods but also avoids their pitfalls. Recent reviews have provided a comprehensive description of these methods for fabrication of inorganic hollow spheres, from multilevel hollow spheres to non-spherical, even one-dimensional (1D) hollow structures.^{4,31–34}

In order to avoid overlapping reviews, this article will mainly focus on the syntheses and applications of inorganic hollow spheres rather than any non-spherical and 1D hollow structures. We will first discuss the syntheses of inorganic hollow spheres with polymer, inorganic nonmetal, and metal-based hard templates and small-molecule or oligomer

emulsion, surfactant micelle-based soft-templates, and template-free approaches. For each method, we provide critical comments based on our knowledge and related research experience. Then we will introduce some important applications of the inorganic hollow spheres (0D) and two-dimensional (2D) and three-dimensional (3D) arrays of inorganic hollow spheres. Considering the rapidly expanding body of literature in the field, the list of examples provided in this review is by no means exhaustive, some excellent papers reporting novel approaches and applications are even omitted. Representative works were selected from the most recent literature available, with exceptions made only for special cases. The intent is to give the readers a critical discussion of the syntheses and applications of inorganic hollow spheres. Finally, we conclude this review with some perspectives on the future research and development of inorganic hollow spheres.

2. Hard template strategy

Hard templates are widely used to fabricate inorganic hollow spheres. Many compounds, such as polymeric, inorganic nonmetallic, and metallic particles, can be used as hard templates. The final shape and size of the inorganic hollow sphere are essentially dependent upon the templates.

2.1 Polymer template-based methods

Templating against polymer colloids is probably the most common approach to produce hollow spheres. Two methods in particular are used to fabricate hollow spheres with homogeneous, dense layers. One is templating against colloid polystyrene (PS) and its derivatives as the particles to fabricate SiO_2 ,³⁵ SnO_2 ,³⁶ magnet (ccp-Co, hcp-Co, Co_3O_4 , a-Fe, Fe_3O_4 and a- Fe_2O_3),^{37,38} metal–metalloid Ni–B,³⁹ Ni(OH)_2 ,⁴⁰ and others.^{41,42} In its typical procedure, the PS template particles are coated in solution either by controlled surface precipitation of inorganic molecule precursors (SiO_2 , TiO_2 , *etc.*) or by



Xiaosheng Fang

the Department of Materials Science, Fudan University, China. His current research topic is the controlled fabrication, novel properties and optoelectronic applications of semiconductor nanostructures, with a focus on II–VI inorganic semiconductor nanostructures-based optoelectronic devices.

Xiaosheng Fang received his PhD degree from the Institute of Solid State Physics, Chinese Academy of Sciences in 2006, under the supervision of Professor Lide Zhang. He joined the National Institute for Materials Science (NIMS), Japan, as a JSPS postdoctoral fellow and then the International Center for Young Scientists (ICYS)—International Center for Materials Nanoarchitectonics (MANA) as a researcher. Currently, he is professor at



Limin Wu

Limin Wu received his PhD degree from Zhejiang University in 1991. He worked as a lecturer then an associate professor from 1991 to 1994. He worked as a visiting professor at Pennsylvania State University and Eastern Michigan University from 1994 to 1999. He joined Fudan University in 1999, where he currently is “Changjiang Scholar” Professor awarded by the Ministry of Education of China. His current research interests include synthesis, assembly and photoelectric properties of organic–inorganic nanoparticles, hollow inorganic particles, development of functional coatings and films.

direct surface reactions utilizing specific functional groups on the cores to create core-shell composites. The PS template particles are then removed by selective dissolution in an appropriate solvent or by calcination at elevated temperature in air, leaving behind hollow spheres. Bourgeat-Lami *et al.* synthesized PS latex particles bearing silanol groups on the surface *via* emulsion polymerization using 3-(trimethoxysilyl) propyl methacrylate as a functional co-monomer.⁴³ These PS colloids were then transferred into aqueous ethanol solution by solvent exchange, wherein the co-condensation of the silanol groups with tetraethoxysilane (TEOS) was carried out *via* an ammonia-catalyzed sol-gel process, causing composite particles with PS cores and SiO₂ shells. Hollow SiO₂ spheres were obtained by thermal degradation of the PS cores at 600 °C. Yang and Lu *et al.* first described a new approach to the generation of inorganic hollow spheres using a template of the core-shell PS gel particles synthesized by an inward sulfonation with concentrated sulfuric acid.⁴⁴ They also successfully prepared double-shelled TiO₂ spheres with a kind of special hollow spheres polymer as a template.^{45,46} This special hollow template composite was composed of hollow PS spheres containing a thin hydrophilic inner layer and transverse channels of poly (methyl methacrylate)-poly (methacrylic acid) (PMMA-PMA). As shown in Fig. 1, when the hollow sphere template was first treated with sulfuric acid, the sulfonation took place in the exterior shell surface, the interior shell surface, and the transverse channels. This sulfonation of the hollow spheres enhanced the hydrophilicity of the spheres and provided a suitable graft surface for adsorption or forming complexes with a large variety of functional components, such as metal ions, metal oxide precursors, and organic precursors. Using TiO₂ as an example, the sulfonated hollow spheres were immersed into a Ti(OBu)₄ sol to coat a layer onto both the inner and outer interfaces of the hollow spheres. The existence of PMMA-PMA transverse channels on the PS shell acted as the entrance for the TiO₂ sol. The double-shelled TiO₂ hollow spheres were obtained after the intermediate PS layer was removed by a solvent. Following a similar procedure, the same authors successfully prepared carbon,⁴⁷ TiO₂, BaTiO₃ and SrTiO₃ hollow spheres.⁴⁸

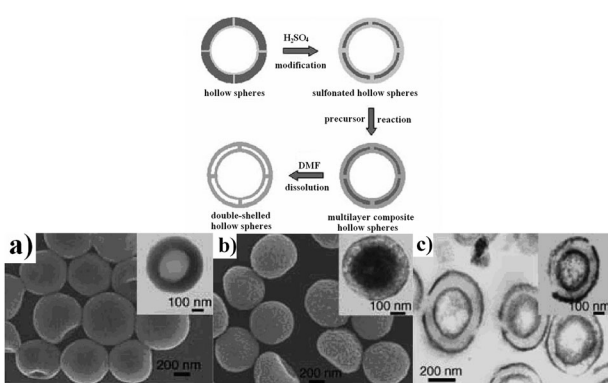


Fig. 1 Illustration of the formation of double-shelled hollow spheres. (a) The sulfonated polymer hollow sphere templates; (b) titania composite hollow spheres; (c) doubled-shelled titania hollow spheres. Reprinted with permission from ref. 45. Copyright 2005 Wiley-VCH.

Ma *et al.* used porous polystyrene-divinyl-benzene (PS-DVB) spheres as templates to synthesize multi-shelled spheres and sphere-in-sphere structures by modifying the post-calcination process.⁴⁹ The temperature during the preheating process directly affects the final structures of TiO₂ spheres. Except for using PS and its derivatives as templates, melamine formaldehyde can also be used to prepare hollow spheres based on noble metal oxides and magnetic oxides.⁵⁰

Another method, termed the layer-by-layer (LbL) self-assembly technique, has become an attractive topic of investigation ever since it was first developed by Caruso *et al.*^{51,52} The principle of this process is based on the electrostatic association between alternately deposited, oppositely charged species. Multilayered shells are assembled onto submicrometer-sized colloidal PS particles by the sequential adsorption of polyelectrolytes and oppositely charged nanoparticles. Upon calcination of the obtained core-shell particles, uniform-sized hollow spheres of various diameters and wall thicknesses can be generated from a variety of inorganic materials, including SiO₂,^{51,52} TiO₂,⁵³ Mn₂O₃,⁵⁴ zeolite,⁵⁵ and other materials.⁵⁶

In polymer template-based methods for preparation of inorganic hollow spheres, the biggest advantage is that the polymer templates are easily prepared with controllable sizes and surface functional groups, thus many hollow spheres of nonmetallic oxides, metallic oxides, and even metals can be fabricated through this approach. However, the preparation processes can require a lot of energy and time. First, multi-step processes are required for the synthesis of core-shell composite particles, *e.g.*, the surface-functionalization of templating particles and the exchange of solvent/coating reaction in the templating particle approach and repeated adsorption/centrifugation/washing/redispersion cycles in the LbL method. Second, in order to obtain hollow spheres from core-shell composite particles, removing the core particles by selective dissolution in an appropriate solvent or by calcination at elevated temperature in air is indispensable.

Recently, Wu *et al.* reported a one-step process of fabricating monodisperse hollow SiO₂ and TiO₂ spheres. This means the formation of the inorganic shells and dissolution of core polymer particles occurs in the same medium (Fig. 2).^{57–60} In this method, monodisperse, positively charged PS beads were prepared by dispersion polymerization using cationic monomer 2-(methacryloyl) ethyltrimethylammonium chloride as co-monomer, which ensures the resulting silica or titania nanoparticles from the hydrolysis and condensation of TEOS or tetra-n-butyl titanate could be rapidly captured by PS beads

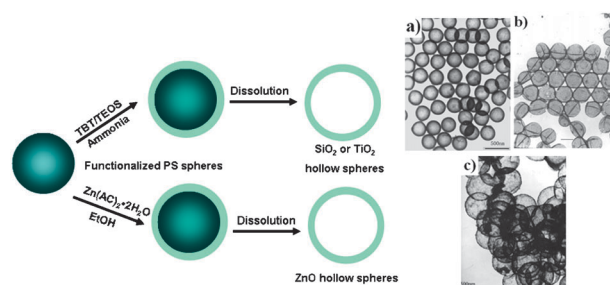


Fig. 2 Schematic illustrations of SiO₂ (a), TiO₂ (b) and ZnO (c) hollow spheres prepared *via* one-step process.

via electrostatic interaction in aqueous ammoniacal alcohol medium at 50 °C. Very interestingly, the PS beads are “dissolved” into PS macromolecule chains or their aggregates subsequently, even synchronously, in the same medium, and are further diffused out gradually through the silica or titania shells since the silica or titania shells prepared by the Stöber method are usually porous, directly forming hollow SiO_2 or TiO_2 spheres. Neither additional dissolution nor calcination processes are needed to remove the PS cores. If negatively charged PS beads are used as templates, then ZnO or even Ag/SiO_2 double-shelled hollow spheres could also be prepared based on the one-step method.^{61,62} If this coating process occurs under acidic circumstances, PS/ SiO_2 hybrid hollow spheres and PS/rare-earth-doped nanocrystals (LaF_3 ; Eu^{3+} , LaF_3 ; Ce^{3+} – Tb^{3+} , and YVO_4 ; Dy^{3+}) hybrid hollow spheres could be directly obtained *via* a one-pot synthesis, in which the PS macromolecular chains diffused from core into the voids between inorganic nanoparticles driven by the strong capillary force to form hybrid shells. This organic–inorganic hybrid shell is expected to improve the mechanical properties of inorganic hollow spheres.^{63,64}

2.2 Inorganic nonmetallic template-based methods

Inorganic nonmetallic templates mainly include carbon and silica particles. Carbon spheres appear to be particularly suitable for templating due to their rich reactive groups and ease of removal. Many uniform micro/nano-sized hollow spheres of metallic oxides such as VO_2 ,⁶⁵ Gd_2O_3 : Ln (Ln = Eu^{3+} , Sm^{3+}), Ga_2O_3 , NiO , MnO_2 ⁶⁶ and so on,⁶⁷ have been fabricated using carbonaceous polysaccharide spheres as the templates. The surfaces of the carbonaceous microspheres, prepared from saccharide starting materials by dehydration under hydrothermal conditions, are hydrophilic and functionalized with –OH and C=O groups. Upon dispersal of the carbonaceous microspheres in metal salt solutions, the functional groups on the surface layer are able to bind metal cations through coordination or electrostatic interactions. In the subsequent calcination process, the surface layers incorporating the cationic metal ions are condensed and cross-linked to form oxide hollow spheres. For example, Yang and co-workers reported that hollow Gd_2O_3 : Ln (Ln = Eu^{3+} , Sm^{3+}) microspheres with diameters of about 300 nm were successfully fabricated by using carbon spheres as templates.⁶⁸ As shown in Fig. 3a, when the precipitation agent, urea, was dissolved in water, it decomposed into CO_2 and OH^- , coupled with a large number of –OH bonds on the surfaces of the carbon spheres. In the coating process, Gd^{3+} and Ln^{3+} were easily precipitated on the surfaces of carbon spheres. Then the high crystallization of Gd_2O_3 : Ln (Fig. 3b) was formed and the carbon spheres were removed at a calcination temperature of 700 °C. This fabrication process involves neither organic compounds nor etching agents.

Li and co-workers prepared Ga_2O_3 and GaN semiconductor hollow spheres, ranging from 100 nm to 1.5 μm in size, by adsorption of metal cations to the surface layer of hydrophilic carbon (carbonaceous polysaccharide) spheres with copious –OH groups, followed by calcination in air.^{69,70} They then extended this method to prepare hollow spheres from a wide

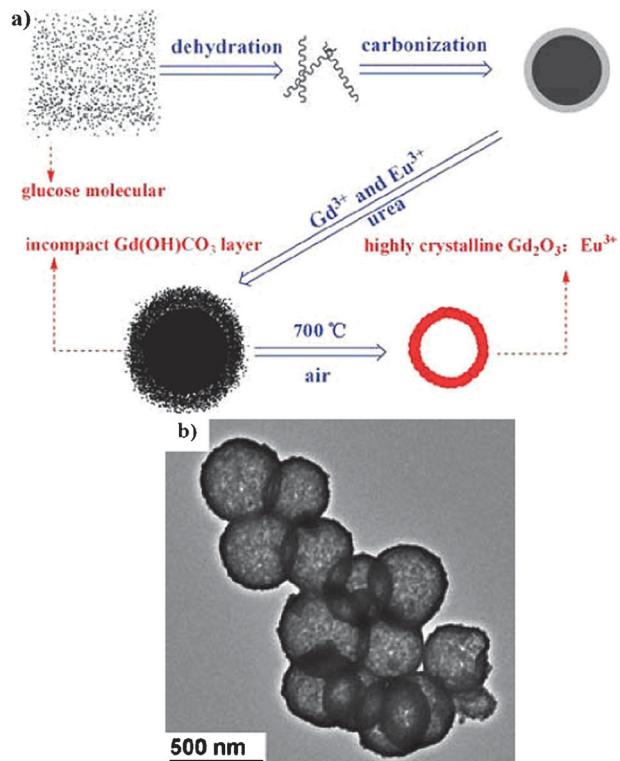


Fig. 3 (a) Schematic illustration of the formation of carbon spheres, the core-shell structured precursor and hollow Gd_2O_3 : Ln spheres. (b) TEM image of hollow Gd_2O_3 : Eu^{3+} spheres. Reprinted with permission from ref. 68. Copyright 2010 Royal Society of Chemistry.

range of metal oxides, including main group metal oxides (Al_2O_3 , SnO_2), transition metal oxides (ZrO_2 , TiO_2 , CoO , NiO , Cr_2O_3 , Mn_3O_4), and rare earth oxides (La_2O_3 , Y_2O_3 , Lu_2O_3 , CeO_2).⁷¹ Suslick *et al.* reported a sonochemical fabrication of crystalline hollow hematite (Fe_2O_3) using carbon nanoparticles as a spontaneously removable template for nanosized hollow core formation.⁷²

In order to simplify the preparation of inorganic hollow spheres with carbon templates, Thomas *et al.* described a simple one-pot hydrothermal approach to the preparation of hollow spheres from crystalline metallic oxides such as Fe_2O_3 , Ni_2O_3 , Co_3O_4 , CeO_2 , MgO , and CuO .⁷³ As indicated in Fig. 4, various metal salts were dissolved in water with carbohydrates, and the mixtures were heated to 180 °C in an autoclave. During the hydrothermal treatment, carbon spheres were

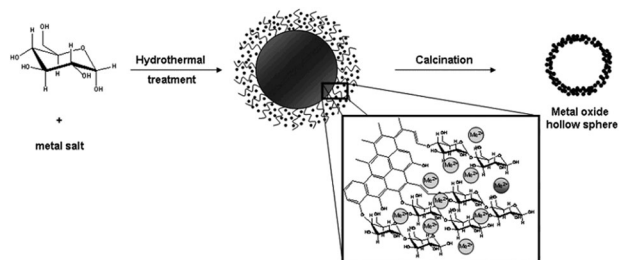


Fig. 4 Schematic illustration of the synthesis of metal oxide hollow spheres from hydrothermally treated carbohydrate/metal salt mixtures. Reprinted with permission from ref. 73. Copyright 2006 American Chemical Society.

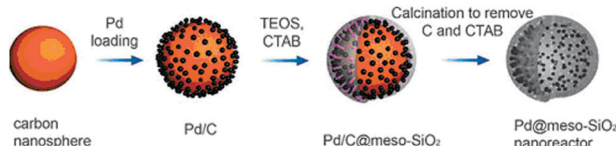


Fig. 5 Synthesis route to the composite nanoreactor. Reprinted with permission from ref. 76. Copyright 2010 Royal Society of Chemistry.

formed *in situ* with metal ions incorporated into their hydrophilic shell. The removal of carbon *via* calcination left behind hollow metallic oxide spheres. Following this method, ternary metal oxide hollow spheres (CoFe_2O_4) were also prepared.⁷⁴

In addition, the hollow shells of crystalline porous metal oxides such as $\gamma\text{-Al}_2\text{O}_3$, TiO_2 , $\text{MgO}\text{-Al}_2\text{O}_3$, and MgTiO_3 have been nanocast using hollow spheres of mesoporous carbon as hard templates. The metal oxides are fabricated from alkoxide precursors within the pore channels of the carbon templates.⁷⁵

With the help of abundant hydroxyl groups on surfaces of the carbon nanospheres, a composite nanoreactor with mesoporous silica hollow spheres and palladium (Pd) nanoparticles inside was prepared in three steps.⁷⁶ As illustrated in Fig. 5, the Pd nanoparticles, about 5 nm in size, are uniformly distributed on the surfaces of the carbon nanospheres. Using TEOS as the silica source and cetyl trimethylammonium bromide (CTAB) as a soft template, a thin layer of mesoporous silica is coated onto the Pd/C spheres. Calcination of the precursor composite removes the carbon sphere and CTAB, leaving only Pd nanoparticles inside the hollow spheres. Carbon spheres can be used not only as templates but also as the direct reagent, which can considerably simplify the fabrication process. Based on this idea, Chen *et al.* successfully fabricated SiC hollow spheres between solid carbon spheres and silicon vapor.⁷⁷ The diameter of the SiC nanospheres had about 18% shrinkage compared to the carbon nanospheres, which could be attributed to the direct reaction between the carbon-surface and the silicon-vapor.

Silica is another common inorganic metallic template to prepare hollow spheres because it is inexpensive, easily obtainable and controllable in size. There are several inorganic hollow spheres fabricated with silica particles as templates, such as nickel hydrosilicate,^{77–79} carbon,⁸⁰ and palladium.⁸¹ The general procedure involves the coating of silica templates by surface precipitation of suitable inorganic precursors and the removal of the silica templates by etching using an alkaline or hydrogen fluoride. For example, Hyeon *et al.* successfully prepared Pd hollow spheres using mercaptopropylsilyl-functionalized silica particles as templates.⁸² Pd precursor was adsorbed onto the surfaces of the functionalized silica spheres and then reduced by CO at 250 °C to produce Pd metal-coated spheres. Pd hollow spheres were yielded after the removal of the silica templates by etching. Zhao *et al.* reported the fabrication of graphitizable hollow carbon spheres (HCSs) with single shells, deformed shells, double shells, and N-doped shells using silica spheres as templates and benzene as a carbon precursor *via* chemical vapor deposition (CVD).⁸³ The microscopic features and shell thicknesses of the HCSs were found to depend on experimental conditions such as silica sphere diameter, CVD temperature, and duration.

In order to further expand the potential applications of hollow spherical structured materials, it is also important to design shells with unique structures, advanced chemical compositions, and built-in functionalities. For example, Wang *et al.* prepared a novel hierarchical structure of copper silicate (CuSiO_4) hollow spheres with nanotube assembled shells.⁸⁴ The silicon–oxygen bonds of SiO_2 colloidal spheres could be broken to form silicate ions under an alkaline condition. Ammonia was used as the source of OH^- and coupled with Cu^{2+} in the form of complex ions which homogeneously dispersed in solution. SiO_4^{2-} was generated and reacted with Cu^{2+} around the SiO_2 colloidal spheres at the high temperature, forming CuSiO_4 which preferentially deposited on the surface of SiO_2 colloidal spheres. With the reaction proceeding, the SiO_2 colloidal spheres were consumed and more CuSiO_4 was generated from the Cu–ammonia complex ions, causing CuSiO_4 hollow spheres with large specific surface areas and excellent adsorption capabilities (Fig. 6). They went on to develop a versatile method of synthesizing nickel silicate, silica, and silica–nickel composite porous hollow spheres by using silica spheres as templates.⁸⁵ Wan *et al.* synthesized Sn nanoparticle encapsulated elastic hollow carbon spheres (TNHCs).⁸⁶ Polycrystalline SnO_2 was first deposited on the templates of SiO_2 spheres to form uniform shells by the hydrolysis of Na_2SnO_3 . Then SnO_2 spheres were obtained by etching SiO_2 cores with NaOH solutions. The carbon precursor layers were coated on the outer surface of the hollow SnO_2 spheres by the pyrolysis of glucose under hydrothermal conditions. TNHCs were prepared by the carbonization of the carbon precursor shell and the reduction of the inner SnO_2 shells.

Recently, Wang and Yamauchi fabricated Pt spheres with hollow interior and nanospunge shells with high surface areas by using SiO_2 particles functionalized with amino groups as templates.⁸⁷ During the process, the amino groups on the SiO_2 surface played a key role in forming attachment sites for initial Pt seeds and then acted as nucleation sites for the subsequent Pt growth. Furthermore, the average thickness of the Pt shells increased proportionally with increasing amounts of Pt (Fig. 7).

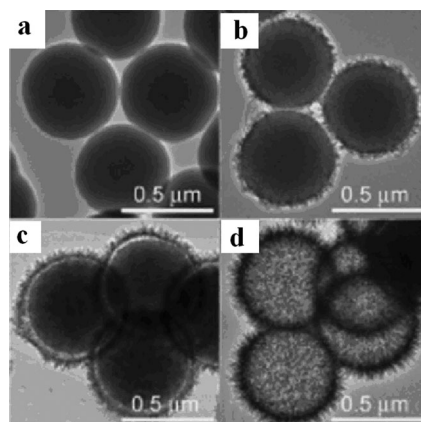


Fig. 6 TEM images of the products collected at 140 °C for different reaction times: (a) 0; (b) 1; (c) 2 and (d) 10 h. Reprinted with permission from ref. 84. Copyright 2008 Royal Society of Chemistry.

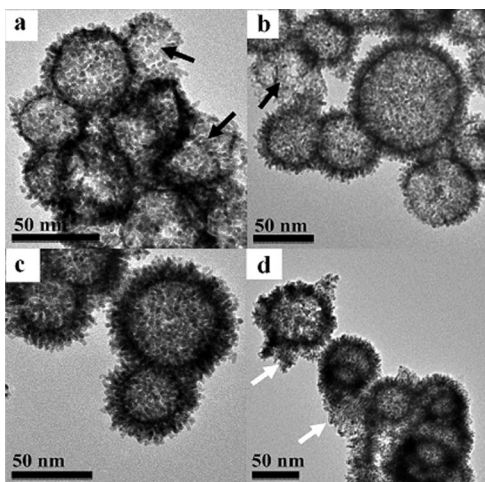


Fig. 7 Various hollow Pt spheres were prepared from precursor solutions containing different Pt amounts. (a) 2.5, (b) 5.0, (c) 7.5, and (d) 10 mL, respectively. The collapse of the hollow structures is indicated by black arrows, while the isolated Pt dendrite (as by-product) is indicated by white arrows. Reprinted with permission from ref. 87. Copyright 2011 Royal Society of Chemistry.

Mesoporous silica spheres are also often used as templates. Su *et al.* demonstrated a new versatile core-shell method of monodisperse crystalline semiconducting ZnS hollow microspheres employing CMI-1 mesoporous silica spheres as templates (2–5 μm in diameter).⁸⁸ The reaction between mesoporous silica spheres functionalized with ethylenediamine molecules that chelated zinc ions and the sulfide reagent in an aqueous solution led to the formation of ZnS. Then ZnS hollow microspheres of around 1–2 μm in diameter were fabricated by etching the mesoporous silica core. Liu *et al.* also synthesized 200–300 μm zeolite hollow spheres with core/shell structures *via in situ* hydrothermal transformation of commercially available mesoporous silica spheres into ZSM-5 crystals of about 200 nm with the assistance of isopropylamine, a weak structure-directing agent for MFI zeolite.⁸⁹

Along side pure carbon or silica particles as inorganic nonmetallic templates, Cheng *et al.* fabricated SiC hollow spheres from a mesoporous SiO_2 –C nanocomposite by taking advantage of microphase separation in the mesoporous silica–carbon nanocomposite.⁹⁰ The SiC shell grew through a carbothermal reduction between the two separated phases, the carbon spheres and the silica-rich matrix. Hollow SiC was formed after oxidation.

Because carbon and silica templates are hydrophilic and functionalized with –OH and other groups on their surfaces, they can provide the following advantages. (1) Cationic materials rather than alkoxides or metal oxide nanocrystals can be used as starting materials. This reduces preparation cost and saves time because alkoxides are sensitive to humidity and monodisperse nanoparticles are not readily accessible. (2) Agglomeration can be avoided because the cations are absorbed onto the surface layer to form a composite shell rather than forming a heterogeneous coating. In all, the carbon spheres are effective templates to prepare the metallic and metallic oxide hollow spheres, while the silica spheres are more used to fabricate metallic and nonmetallic salt hollow spheres.

In addition, the functional groups on the surfaces of the carbon spheres are inherited from the saccharide, so no surface modification or activation steps are required. This greatly reduces the processing steps and thus saves time. As the thickness of the functional surface layer is predetermined by hydrothermal synthesis, the integrity and uniformity of the shells of the final products can be assured.

As a whole, no matter whether inorganic nonmetallic or polymeric beads are used as templates, three steps are indispensable: (i) surface-functionalization/modification of the template particle to acquire favorable surface properties; (ii) coating the templates with designed ceramic shells or their precursors by various approaches; and (iii) selective removal of the templates to leave behind hollow structures by etching in appropriate solvents or by calcination at elevated temperatures. Theoretically, these template strategies can assure the expected monodisperse morphology and size of hollow spheres and can be used to fabricate various kinds of inorganic hollow spheres. Nonetheless, their inherent demerits are also obvious. Not only is the fabrication process complicated and tedious, but also special care must be taken to prevent shell collapse during template removal. For example, when using organic solvents to dissolve polymer templates, swelling of the polymer can rupture the hollow structure, causing shells with unpredictable shapes. When using high temperatures to burn off polymer templates or to crystallize shell particles, escape of gases produced by pyrolysis of the polymer templates and, possibly, shrinkage during the crystallizing or compacting process, often lead to defects such as holes in surfaces of the final hollow spheres. Post-calcination at high temperatures usually causes aggregation and hard dispersion of hollow spheres in media.

2.3 Metallic template-based methods

In contrast to the above mentioned polymer and inorganic nonmetal templates, the key feature of metal-template-based methods is that the metal template itself can act as a reactant in the synthetic process. The template not only plays the role of scaffold and precursor for the shell, but it is also consumed completely during the coating process. This simplifies the preparation process. The morphology, void space, and wall thickness of the hollow structures are all determined directly by the metal templates. Generally, two formation mechanisms, the Kirkendall effect and galvanic replacement, have been used to understand the fundamentals of inorganic hollow spheres synthesized by metallic templates.

2.3.1 Kirkendall effect. Originally, the term “Kirkendall effect” refers to the different atomic diffusive rates of binary elements in metals and alloys under thermally activated conditions. Due to this difference in metal diffusivities, the generation of porosity in the lower-melting component side of the diffusion couple near the interface could create hollow nanostructures.^{91,92} By introduction of oxidation or sulfidation reactions on the external surfaces of metallic nanocrystals, Alivisatos *et al.* first explained the formation of hollow nanocrystals of cobalt (Co) oxide and chalcogenides.⁹³ The Co nanocrystals were chosen as a starting material to

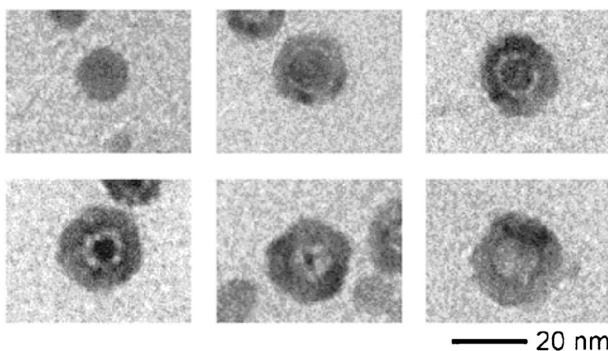


Fig. 8 Evolution of CoSe hollow nanocrystals with time by injection of a suspension of Se in *O*-dichlorobenzene into a cobalt nanocrystal solution at 455 K; from top-left to bottom-right: 0 s, 10 s, 20 s, 1 min, 2 min, and 30 min. The Co : Se molar ratio was 1 : 1. Reprinted with permission from ref. 93. Copyright 2004 American Association for the Advancement of Science.

synthesize the hollow nanocrystals through the reaction of Co colloidal solution with oxygen and either sulphur (S) or selenium (Se). The evolution of hollow morphology could be well illustrated by the reaction of Co nanocrystals with Se (Fig. 8). As the reaction proceeded, more Co atoms diffused out to the shell, and the accompanying transport of vacancies led to growth and merging of the initial voids. This resulted in the formation of bridges of material between the core (Co) and the shells (CoSe). These bridges persisted until the Co was completely consumed. After studying the physics of the nanoscale Kirkendall effect using the formation of cobalt sulfide hollow nanocrystals, they found that performing the reaction at temperatures greater than 120 °C led to fast formation of a single void inside each shell, whereas at room temperature multiple voids were formed within each shell.⁹⁴ This could be attributed to strongly temperature-dependent diffusivities for vacancies. The void formation process was dominated by outward diffusion of Co²⁺ cations. Because the final voids were smaller in diameter than the original Co nanocrystals, it could be inferred that significant inward transport of sulfur anions took place. The team then prepared hollow CdS⁹⁵ and γ -Fe₂O₃⁹⁶ spheres and found that the reaction conditions, such as the diffusion of equal species through an identical composite and the concentration and reactivity of the anion precursor, could have an impact on hollow structures.⁹⁷

Through similar strategies, other inorganic hollow spheres such as hollow CoSe nanoparticles from solution-phase selenization of Co nanoparticles,^{98,99} hollow transition metal phosphide nanoparticles from reactions between metal nanoparticles and trioctylphosphane,^{100,101} hollow magnetic iron oxide nanoparticles from gas-phase oxidation,¹⁰² electron-beam irradiation,¹⁰³ and solution-phase synthesis,¹⁰⁴ have been fabricated. Recently, Peng and Sun reported a facile solution-phase synthesis of monodisperse hollow Fe₃O₄ nanoparticles by controlled oxidation of Fe–Fe₃O₄ nanoparticles.¹⁰⁵ The Fe nanoparticles were not chemically stable and oxidized easily when exposed to air, leaving core-shell Fe–Fe₃O₄ structures with both Fe and Fe₃O₄ in amorphous states. Controlled oxidation of these core-shell nanoparticles in the presence of the oxygen-transfer reagent trimethylamine N-oxide (Me₃NO)

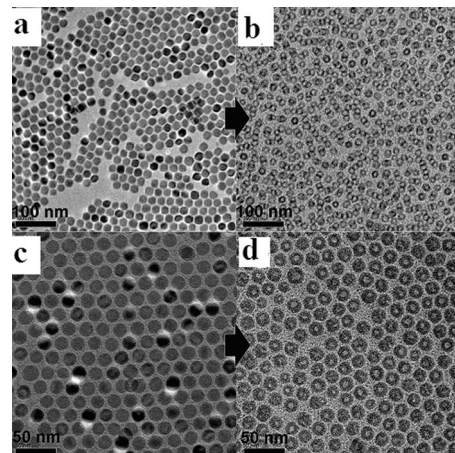


Fig. 9 TEM images showing the changes from solid nanocrystals of 18 nm sized MnO (a) and 20 nm sized Fe₃O₄ nanocrystals (c) to the corresponding hollow oxide nanoparticles ((b) MnO, (d) Fe₃O₄) through the etching process. Reprinted with permission from ref. 106. Copyright 2008 American Chemical Society.

led to the formation of intermediate core-shell-void Fe–Fe₃O₄ and to hollow Fe₃O₄ nanoparticles.

A novel method for the synthesis of uniform hollow oxide nanoparticles was developed based on the Kirkendall effect. It involves a controlled nanoscale etching of MnO and iron oxide nanocrystals (Fig. 9) in the presence of trioctylphosphine oxide and alkylphosphonic acid.¹⁰⁶ In the early stage of the etching process, metal cations were dissolved into the solution by the coordination of alkylphosphonic acid, which increased the vacancy concentration near the surface of the particle. At the same time, phosphorus from the solution diffused to the surface of the particle, filling the vacancies. Continued dissolution of metal cations and supply of phosphorus transformed the outer shell of the nanocrystal from metal oxide to phosphorus oxide. The outward diffusion of metal cations and the accumulation of vacancies inside the shell led to the formation of the void between the core and the shell. The diffusion of metal cations stopped when the composition of the particle became homogeneous. The final amorphous shell, composed of metal, phosphorus, and oxygen, was maintained by the balance of the inward diffusion of phosphorus and the outward diffusion of metal.

Note that the chemical transformation of nanoparticles accompanied by the Kirkendall effect often results in polycrystalline nanoparticle products, while single-crystal hollow structures are rarely obtained. Recently, Alivisatos's group prepared parent-particle shape, single crystallinity and orientation of ZnS hollow nanoparticles through the heteroepitaxial anion exchange reaction with Kirkendall effect.¹⁰⁷ Thin layers of ZnS were grown epitaxially onto the ZnO core through a surface anion exchange reaction, which generated a highly strained interface between the ZnO core and the ZnS shell. To release this interface energy, the ZnO core spontaneously diffused into the ZnS shell, which was finally exchanged with sulfur precursors at the outer shell surface, forming fully converted hollow ZnS nanoparticles (Fig. 10).

To date, although the Kirkendall effect has achieved some success in the preparation of inorganic hollow compounds, it

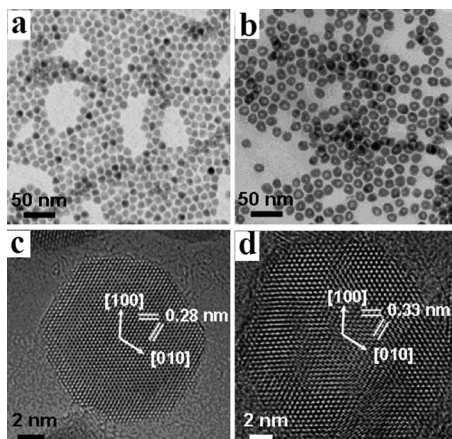


Fig. 10 TEM and HRTEM images of initial ZnO nanoparticles (a, c) and ZnS hollow nanoparticles obtained after anion exchange (b, d). Reprinted with permission from ref. 107. Copyright 2009 American Chemical Society.

is limited to a small number of well-defined nanoscale metallic compounds. The configuration radii of the hollow spheres so obtained are usually indistinct compared to polymer and nonmetallic templates. The formation of the nanoscale Kirkendall effect is still at odds with the phenomenological and ideal model studies. Questions remain regarding the effect's exact mechanism. Thus more comprehensive studies on various kinds of compounds and sizes would be much appreciated to understand the enthralling process.

2.3.2 Galvanic replacement. Galvanic replacement reaction provides a remarkably simple and versatile route to metal nanostructures with controllable hollow interiors and porous walls. The key step of this process involves a replacement reaction between a suspension of more active metal templates and a salt precursor containing a relatively less active metal. Xia *et al.* first described a general approach to the generation of nanoscale hollow metal structures (Au, Pt, Pd) with well-defined void spaces and homogeneous, highly crystalline walls by reacting solutions of appropriate salt solutions with solid templates of a more reactive metal.^{108,109} The major steps involved in this process are shown in Fig. 11, with the gold/silver combination as an example. Silver nanoparticles could be oxidized to silver ions when mixed with an aqueous HAuCl₄ solution. The elemental gold should be confined to the vicinity of the template surface. Then they nucleate and grow into small clusters, and eventually evolve into a shell-like structure around the silver template. The thin shell formed in the early stage was incomplete, and so it was possible for HAuCl₄ and AgCl to diffuse across this layer until the silver template was completely consumed. When the reaction continued with refluxing at an elevated temperature, the wall of each gold shell would be reconstructed into a highly crystalline structure.

Cobalt nanoparticles were even used as templates in the preparation of hollow nanospheres of Ag,¹¹⁰ Pt,¹¹¹ Au,¹¹² and bimetallic AuPt,¹¹³ through galvanic replacement reaction. Galvanic replacement reaction can also be used to fabricate more morphologically complex hollow spheres, such as Pt hollow nanospheres with wall thicknesses of 25 nm and an

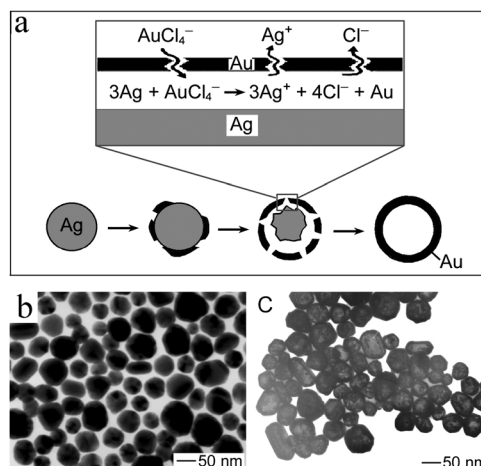


Fig. 11 (a) Schematic illustration of the experimental procedure that generates gold nanoshells by templating against silver nanoparticles. (b) TEM image of silver nanoparticles prepared using the polyol process. (c) TEM image of gold nanoshells obtained by reacting these silver nanoparticles with an aqueous HAuCl₄ solution. Reprinted with permission from ref. 109. Copyright 2003 Wiley-VCH.

urchin-like structure. This increases the effective surface-to-volume ratios for hollow nanostructure nanocatalysis and nanobiosensor applications.¹¹⁴ Recently, bimetallic NiPt hollow spheres with controlled sizes and compositions were also synthesized by a facile wet chemical process combined with galvanic replacement.¹¹⁵

When comparing galvanic replacement reaction to the Kirkendall effect, galvanic replacement reaction does not require additional surface functionalization either, and moreover, it can be employed as a general route to fabricate hollow structures in a variety of shapes and sizes, but obviously, only for metallic hollow structures.

3. Soft template-based strategies

Soft template-based methods hold appeal because the templates are relatively easy to remove.^{116–120} However, the morphology and monodispersity of the as-prepared hollow products are usually poor due to the deformability of the soft templates. Controlling monodispersity and spherical morphology of the inorganic hollow structures is the most challenging part of this technique. Imhof *et al.* successfully synthesized monodisperse micrometre-sized SiO₂ hollow spheres by templating against low-molecular-weight polydimethylsiloxane (PDMS) silicone O/W emulsion droplets with diameters in the range of 0.6–2 µm.^{121,122} Feldmann *et al.* synthesized nanoscale La(OH)₃ hollow spheres exhibiting outer diameters of 11–30 nm and inner cavities of 2–17 nm in W/O microemulsion containing *n*-dodecane as the nonpolar oil phase, CTAB as the surfactant and 1-hexanol as the co-surfactant.¹²³ Adjustment of the water to surfactant ratio of the underlying micellar system and the size of the relevant micelles influences the outer diameter and cavity size. Silver spheres of less than 50 nm in diameter with a wall thickness of 3–5 nm and an inner cavity of 10–15 nm were also realized in this way.¹²⁴ More complex structural inorganic hollow spheres, such as hollow cage-like silica spheres loaded with superparamagnetic

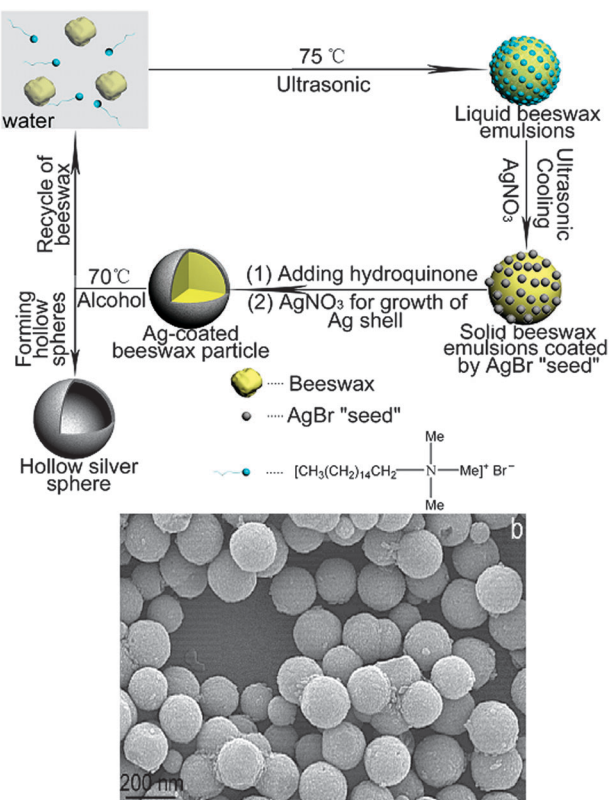


Fig. 12 Schematic of the formation of hollow silver spheres using phase-transformable emulsion as the template. Reprinted with permission from ref. 126. Copyright 2008 American Chemical Society.

iron oxide nanoparticles incorporated in their macroporous shells, have also been prepared *via* the oil-in-diethylene-glycol microemulsion method.¹²⁵

Recently, Wu *et al.* successfully prepared monodisperse and size-tunable hollow Ag spheres with phase-transformable emulsions composed of natural beeswax as templates (Fig. 12).¹²⁶ First, a mixture of beeswax and CTAB aqueous solution containing KBr was heated to 75 °C to produce molten-state beeswax, followed by an ultrasonic process to obtain monodisperse, stable emulsion droplets of beeswax. A small amount of AgNO₃ solution was added to form negatively charged AgBr “seeds” which were adsorbed onto the positively charged surfaces of droplets through electrostatic attraction. The AgBr seeds were then reduced to Ag nanoparticles and bound to the solidified beeswax particles. Because the Ag nanoparticles on the beeswax cores could act as catalysts and significantly accelerated the reduction process while the reduction of AgBr in continuous phase was metastable, and normally very slow, more Ag was deposited onto the surfaces of beeswax particles as more AgNO₃ solution was added. This led to dense, monodisperse Ag-coated beeswax spheres. Because natural beeswax has a relatively low phase-transformable temperature from solid to liquid ($T_m = 62\text{--}67$ °C), the beeswax cores were easily emigrated from inside to outside when heated to 70 °C, leaving behind well-defined hollow Ag spheres.

Han *et al.* fabricated hollow SiO₂ spheres using water-*n*-heptane/CTAB nanoemulsions and compressed CO₂ as a

template.¹²⁷ During the preparation process, heptane droplets with TEOS (oil phase) were dispersed in the aqueous phase with the aid of the surfactant. At the same time, there existed cylindrical micelles of the surfactant in the aqueous phase. Addition of the compressed CO₂ into the emulsion caused the dispersed oil droplets to become smaller and more uniform. The hydrolysis of TEOS occurred around the micelles near the oil/water interfacial region. The oil droplets formed the cores of the spheres, and the cylindrical micelles acted as templates for the formation of the mesopores in the SiO₂ shells. SiO₂ hollow spheres with ordered mesoporous shells were formed after removing the oil and surfactant by washing and calcination.

Surfactant molecules in aqueous solution can also self-assemble to form the micelles and closed-bilayer aggregates such as vesicles (also referred to as organized molecular assemblies) or dynamic nanostructures of surfactant molecules. These micelles or vesicles have been used as the templates to prepare hollow spheres, such as SiO₂,^{128–130} ZnO,¹³¹ GuS,¹³² and other materials.¹³³ Wang and co-workers first successfully synthesized single-, double-, triple-, and quadruple-shelled GuO₂ hollow spheres with CTAB multi-lamellar vesicles as soft templates at 60 °C, as shown in Fig. 13.¹³⁴ The concentration of the CTAB surfactant was found to be capable of adjusting the structures of these Cu₂O hollow spheres. Further, they simplified the process to synthesize Cu₂O hollow spheres with uniform double-wall structures at room temperature and without the addition of sodium hydroxide. The double-wall structure and size of Cu₂O hollow spheres was not found to change with increasing concentrations of CTAB.¹³⁵

This method can be extended to the utilization of poly(vinylpyrrolidone) as a vesicle template in the syntheses of various hollow structures such as VO₂,¹³⁶ BaWO₄,¹³⁷ SiO₂,¹³⁸ Co₃O₄ and PbO₂ spheres.¹³⁹ For example, based on the template of poly(vinylpyrrolidone), γ-Fe₂O₃ hollow spheres with multilevel interior structures were fabricated *via* the heterogeneous contraction approach by fast heating their gel precursors.¹⁴⁰ The structure of the hollow spheres could be controlled for the formation of solid, hollow to core-in-hollow-wall, double-wall

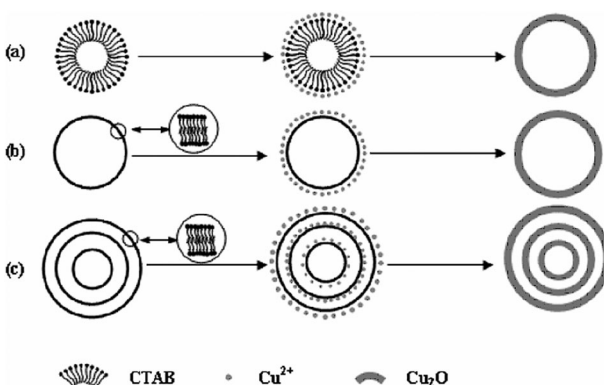


Fig. 13 The formation of different Cu₂O hollow structures in the presence of CTAB template: (a) micelle, (b) single-lamellar vesicle, (c) multilamellar vesicle. Reprinted with permission from ref. 134. Copyright 2007 Wiley-VCH.

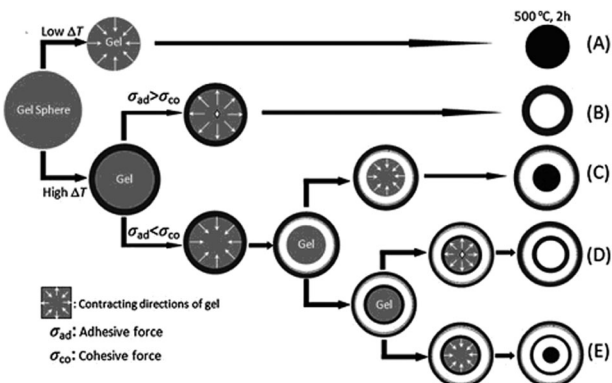


Fig. 14 Illustration for the formation mechanism of solid (A), hollow (B), core-in-hollow-wall (C), double-wall hollow (D) and core-in-double-hollow-wall (E) spheres. Reprinted with permission from ref. 140. Copyright 2010 Royal Society of Chemistry.

hollow, and core-in-double-hollow-wall spheres by adjusting the heating rate of the calcination as shown in Fig. 14.

Very recently, Che *et al.* successfully prepared novel SiO_2 mesoporous crystal spheres with polyhedral hollows and the reverse multiply twinned bicontinuous double diamond mesostructure as seen in Fig. 15.¹⁴¹ The hollow SiO_2 mesoporous crystal spheres were synthesized using amino acid-derived, anionic, amphiphilic *N*-stearoyl-L-glutamic acid as the template, 3-aminopropyltrimethoxysilane as a costructure directing agent, and TEOS as the silica source in the presence of the nonionic surfactant $\text{C}_{16}\text{H}_{31}(\text{OCH}_2\text{CH}_2)_{10}\text{OH}$. The formation of vesicles with low-curvature lamellar structure, which was self-assembled by amphiphilic carboxylic acid molecules in the presence of a nonionic surfactant and the lamellar-to-cubic shell transformation of vesicles, gave a

reverse multiply twinned mesoporous shell while maintaining the hollow shape.

Soft templates include not only emulsion droplets, surfactants, other supramolecular micelles, and polymer vesicles,¹⁴² but also polymer aggregates and gas bubbles;^{143–146} more examples can be found in a previous review.³²

Compared to hard template-based methods, soft template-based methods not only eliminate the cores easily by gentle evaporation or dissolution in solvents, but also the liquid droplet templates still allow facile and efficient introduction of therapeutic and biologic active species inside the spheres. However, although some infusive progresses in controlling the size, uniformity and microstructure of the inorganic hollow spheres in the soft templates have been made in the past several years, this challenge is still serious and hard to overcome in most cases. This is attributed to the characteristics of soft templates. For example, the emulsion droplets are thermodynamically unstable, and the precursor of shell materials can initially exist in either the continuous phase or the droplet phase or both phases; the structure and stability of the supramolecular micelles/vesicles as soft templates are affected by many factors such as the solvent polarity, pH value, and the ionic strength of the solution.

4. Template-free strategy

As discussed above, although template methods are arguably the most effective and certainly the most common means of synthesizing hollow inorganic spheres on the micro and nano scales, some inherent disadvantages have proven very difficult to overcome. For example, in most hard template-based methods, removal of the template by either thermal or chemical means is very complicated and energy consuming. In soft template-based methods, the morphology and monodispersity of the hollow spheres are very difficult to control. Recently, the Ostwald ripening process has been proposed as a template-free strategy and is used more and more to fabricate inorganic hollow spheres. The basic principle of the inside-out Ostwald ripening process is that the larger crystals grow from those of smaller size, which have higher solubility than the larger ones.¹⁴⁷ Within a colloidal aggregate, smaller, less crystallized, or less dense crystallites will dissolve into the liquid phase as a nutrient supply for the growth of larger, better crystallized, or denser ones. When the crystals grow in solution, the concentration of growth units varies across the mother solution, due to the size difference of resultant nanocrystals.^{148,149} With the driving force of the minimization of surface energy, metastable nanoparticle aggregates occur first due to the reduction of supersaturation in solution. Once the particles with different sizes are attached to each other, the large particles begin to grow, drawing from smaller ones. Voids gradually form and grow in the cores of large aggregates, and the shell thickness increases owing to the outward diffusion of solutes through the permeable shell.⁴

The inside-out Ostwald ripening mechanism has been used to synthesize hollow spheres of a wide range of materials, such as, Fe_3O_4 ,^{150,151} SnO_2 ,¹⁵² Co ,¹⁵³ Sb_2S_3 ,¹⁵³ Bi_2WO_6 ,¹⁵⁴ TiO_2 ,^{155–158} and other materials.^{159–162} For example, Zeng and coworkers reported a “one-pot” method of preparing

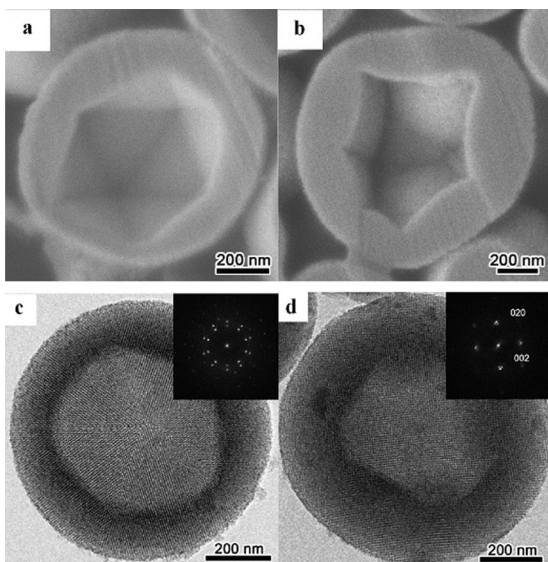


Fig. 15 (a and b) Cross-sectional SEM images of silica mesoporous crystal spheres with polyhedral hollows; (c) HRTEM image taken from the common [110] direction of the decahedron shape; (d) HRTEM image of a Wulff polyhedron taken from the [100] direction. Reprinted with permission from ref. 141. Copyright 2011 American Chemical Society.

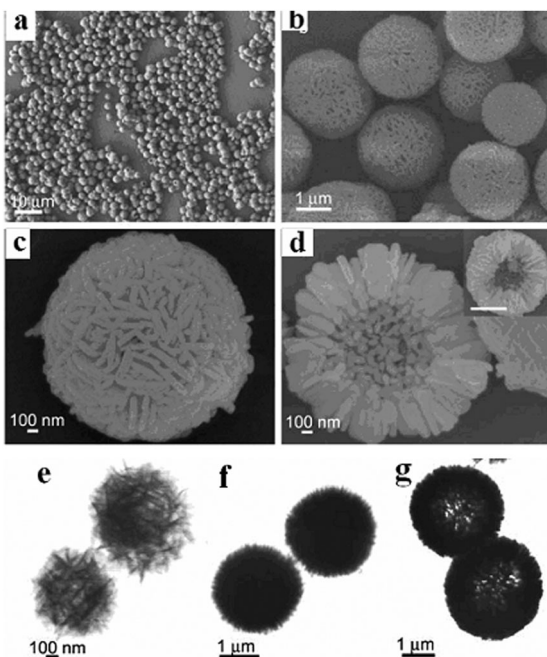


Fig. 16 SEM (a, b, c, d) and TEM images of $\text{Ni}(\text{OH})_2$ prepared at 100 °C with different experimental times: (e) 30 min; (f) 1 h; (g) 24 h. Reprinted with permission from ref. 165. Copyright 2005 Royal Society of Chemistry.

hollow anatase TiO_2 spheres with diameters of 0.2–1.0 μm via the inside-out Ostwald ripening in TiF_4 solution.¹⁶³ The reduction of the overall surface energies could provide the driving force for Ostwald ripening within all the particles. With respect to hollowing, no apparent driving force could be easily identified.¹⁶⁴ Wang *et al.* prepared a hierarchical structure of $\text{Ni}(\text{OH})_2$ hollow microspheres with $\beta\text{-Ni}(\text{OH})_2$ nanosheets as the *in situ* building units (Fig. 16a–d).¹⁶⁵ NiO hollow spheres were successfully synthesized by thermal decomposition of the as-synthesized $\text{Ni}(\text{OH})_2$ hollow spheres at 600 °C for 2 h. The formation process of $\text{Ni}(\text{OH})_2$ hollow microspheres could be divided into three obvious stages. In the first stage, the precipitated $\text{Ni}(\text{OH})_2$ crystals assembled into loosely attached aggregates with diameters of 800–900 nm. With increasing reaction time, the aggregates continuously grew in size and density to form spheres with solid cores. Finally, an interior cavity was gradually formed via a core evacuation process, through a mechanism similar to Ostwald ripening (Fig. 16e–g). Wang *et al.* further reported a hierarchical and porous structure of Ni hollow microspheres with Ni nanoparticles as the *in situ* formed building units which were fabricated by a novel, hydrothermal redox method with $\text{Ni}(\text{OH})_2$ as the precursor.¹⁶⁶

Also, the hollow spheres produced from the self-templated formation have recently been further elaborated.^{167,168} The term “localized Ostwald ripening” is used to describe the preferential dissolution of the particle interior. Yu *et al.* prepared a wide range of hollow spheres including calcium carbonate, strontium tungstate, TiO_2 , SnO_2 , $\text{CuO}/\text{Cu}_2\text{O}$ and so on.^{169–171} With increasing reaction time, the surface layer first transformed to a thermodynamically more stable form (*e.g.*, crystallization), as the supersaturation fell in the

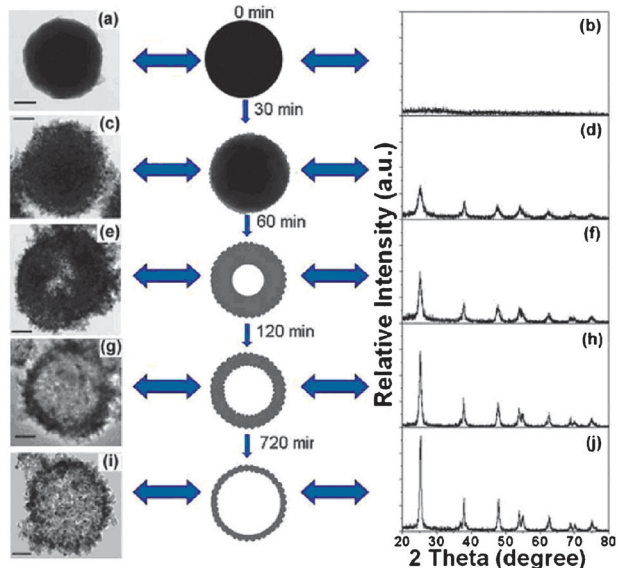


Fig. 17 Schematic illustration of formation of anatase TiO_2 hollow spheres (at $R = 1$). The left and right panels respectively show the TEM images and corresponding XRD patterns of the intermediate products prepared at 180 °C for 0 (a, b), 30 (c, d), 60 (e, f), 120 (g, h) and 720 min (i, j), respectively. The scale bar is 100 nm. Reprinted with permission from ref. 172. Copyright 2010 Royal Society of Chemistry.

surrounding solution. Thus an ultrathin shell of less-soluble crystalline phase was formed on the amorphous solid spheres. As a result, the amorphous core would have a strong tendency to dissolve and diffuse out through the shell because it remained out of equilibrium with the surrounding solution. Furthermore, they prepared mesporous anatase-phase TiO_2 hollow spheres with high photocatalytic activity by hydrothermal treatment and self-transformation of amorphous TiO_2 solid spheres in an NH_4F aqueous solution.¹⁷² Initially (0 min), the precursors were solid spheres with smooth surfaces (Fig. 17a) and in the amorphous state (Fig. 17b). After hydrothermal reaction for 30 min, the diffraction peaks for the crystalline TiO_2 -anatase appeared in the XRD pattern of the product (Fig. 17d). The product was still solid spheres and the surfaces of the spheres, which contained nano-sized crystalline particles, became rough (Fig. 17c). Extending the reaction time to 60 min resulted in an increase in the crystallinity of the samples (Fig. 17f), and the hollowing interiors took place around the centers of the solid spheres (Fig. 17e).

Complex structures, such as core-shells and binary and ternary composite hollow spheres can also be prepared via Ostwald ripening.^{173–176} Zeng and Liu synthesized hollow core-shell oxide and sulfide semiconductor particles.¹⁷⁷ While the original shape of a crystallite aggregate forms the exterior appearance, the route of preorganization of crystallites determines the ultimate interior space structure of the aggregate upon Ostwald ripening. They demonstrated that Ostwald ripening could also be used as a facile wet chemical route to synthesize binary metal oxide nanospheres with additional architecture of interior spaces. The high-quality Sn-doped TiO_2 hollow spheres were prepared with the hydrolysis of

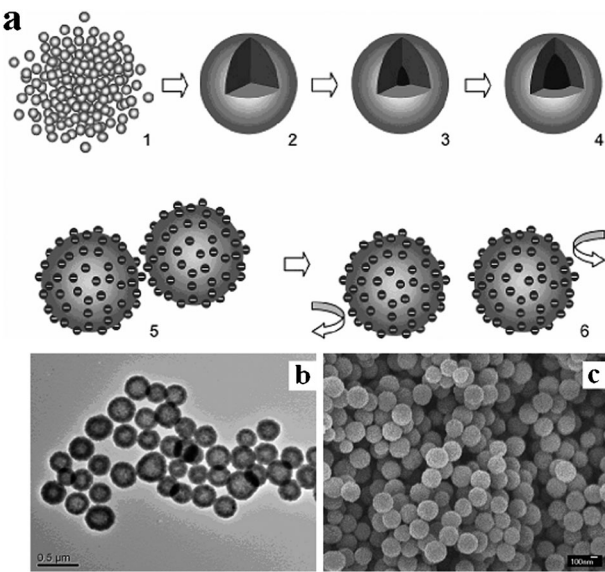


Fig. 18 Formation process of hollow spheres (a); TEM image (b) and SEM image (c) of Sn-doped TiO_2 nanospheres. Reprinted with permission from ref. 178. Copyright 2007 American Chemistry Society.

fluoride salts of both TiF_4 and SnF_4 (Fig. 18). The formation of the hollow sphere was ascribed to an Ostwald ripening process (steps 1–4). The surface-adsorbed fluoride anions prevented the nanospheres from the agglomeration *via* negative repulsive interaction (steps 5 to 6). Furthermore, the fluoride anion overlayer also served as a diffusion boundary to restrain rapid crystal growth and prevent direct fusion among the nanospheres during the ripening. The content of Sn^{4+} in the solid solution obviously influenced the hollowing degree of these nanospheres.¹⁷⁸

Wu *et al.* first reported the successful synthesis of superparamagnetic fluorescent $\text{Fe}_3\text{O}_4/\text{ZnS}$ hollow spheres of under 100 nm in size using corrosion-aided Ostwald ripening.¹⁷⁹ The synthetic procedure was very easy and straightforward. When the monodisperse FeS particles were dispersed in a mixture containing zinc acetylacetone (ZA), PVP, ammonium nitrate, glycol and water, and reacted at 150 °C for 10 h, $\text{Fe}_3\text{O}_4/\text{ZnS}$ hollow spheres were directly obtained. As demonstrated in Fig. 19, ZA hydrolysis at pH 6–9 generated $\text{Zn}(\text{NH}_3)_4(\text{OH})_2$ which further eroded the FeS particles (Fig. 19a) to cause supersaturated Fe_3O_4 and ZnS phase. This phase underwent consequent nucleation and growth around the entire surface stabilized by PVP (Fig. 19b). As time went on, FeS, ZA and water were consumed gradually and the resultant ZnS and Fe_3O_4 molecules decreased in number. The growth rate also decreased, due to the narrowing concentration gap between the molecules in the medium and the equilibrium value needed for growth. The Fe_3O_4 and ZnS formed around the surface of FeS particles, and small particles grew into larger particles, which then coalesced and formed shells (Fig. 19c). Etching did not cease until the FeS core had vanished, finally leaving $\text{Fe}_3\text{O}_4/\text{ZnS}$ hollow spheres (Fig. 19d and e).

Ostwald-ripening-based template-free methods can both resolve the problem of the template removal in hard template-based strategies and provide uniform hollow spheres

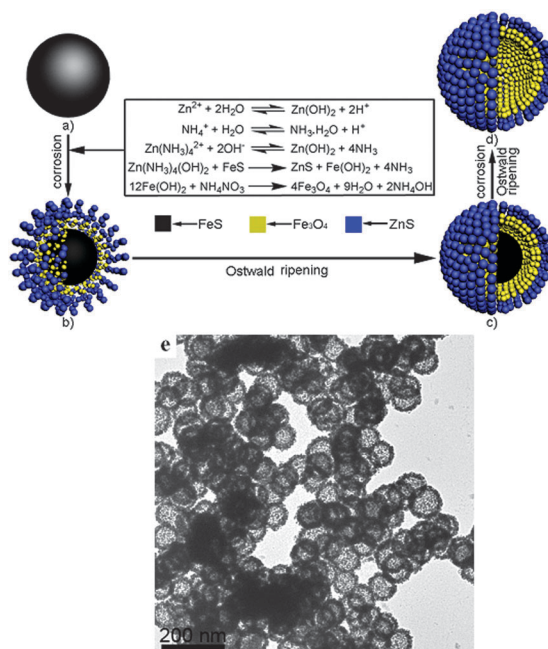


Fig. 19 Schematic diagram of the formation of $\text{Fe}_3\text{O}_4/\text{ZnS}$ hollow spheres and a TEM image of the spheres. Reprinted with permission from ref. 179. Copyright 2009 American Chemical Society.

both in morphology and size that are so difficult to attain *via* soft template-based strategies. However, to date, this strategy has only focused on some special compounds, and no copious fundamental evidences are available in support of this mechanism. More mechanistic studies on the fabrication of inorganic hollow spheres are required to provide deeper fundamental understanding of Ostwald ripening. The representative inorganic spheres and their preparation methods are summarized in Table 1.

5. Applications

The most attractive characteristics of inorganic hollow spheres are their well-defined morphology, their large specific surface area, low density, and the optical, electric, and magnetic properties of their inorganic components. All of these make inorganic hollow spheres superior to other similar materials in applications such as catalysis, lithium-ion batteries, biomedical applications, and gas sensors.^{180,181} We will now introduce some important applications of not only the inorganic hollow spheres themselves (0D), but also the 2D and 3D arrays of inorganic hollow spheres, since more and more much higher-grade assemblies of inorganic hollow spheres have been reported recently.

5.1 Hollow spheres (zero-dimensional, 0D)

Hollow spheres or so called 0D hollow structures have been extensively investigated in their potential applications, especially in catalysts, lithium-ion batteries, biomedical materials and gas sensors. As catalysts, except for Suzuki coupling reactions,⁸⁴ heterogeneous hydrogenation reactions,¹⁸² Sonogashira reactions,^{183,184} aerobic oxidation,¹⁸⁵ many inorganic hollow spheres such as ZnS , C, WO_3 ,¹⁸⁶ TiO_2 ,^{187,188} $\text{CuO}/\text{Cu}_2\text{O}$, ZnO-SnO_2 ,¹⁸⁹ and others¹⁹⁰ occupy photocatalytic

Table 1 Summary of representative inorganic hollow spheres

Structure	Composition	Synthesis methods	Ref.
Single-shelled hollow sphere	SiO_2	LbL self-assembly method based polymer spheres One step method against polymer template Polymer template method O/W emulsion droplets template method Amphiphilic carboxylic acid template method Templating against colloidal crystals Inside-out Ostwald ripening Localized Ostwald ripening Templating against colloidal crystals Silica template method Galvanic replacement reaction Carbon template method Kirkendall effect Ostwald ripening <i>In situ</i> formed carbon template	52 57 43 121 141 36 163 172 36 82 109 69, 70 93 177 73
	TiO_2		
	SnO_2		
	Pd		
	Au, Pt, Pd		
	Ga_2O_3 , GaN		
	CoO , CoS		
	ZnS , Co_3O_4		
	Fe_2O_3 , Ni_2O_3 , Co_3O_4 , CeO_2 , MgO , CuO		
	Fe_3O_4	Kirkendall effect	105
	Ag	Phase-transformable emulsion method	126
	ZnS	Silica template method	88
	Gd_2O_3 : Ln (Ln = Eu ³⁺ , Sm ³⁺)	Carbon template method	68
	NiPt	Wet chemical process combined with galvanic replacement	115
Multi-shelled hollow sphere	TiO_2	Polymer template method	45
	Carbon, Carbon/N	Silica template method	83
	CuO_2	CTBA vesicles template method	134
	Co_3O_4	Self-assembly combined with soft template method	203
Hierarchical hollow sphere	Ni(OH)_2	Inside-out Ostwald ripening	165
	CuSiO_4	Silica template method	84
	WO_3	Template-free method	186
Binary composite hollow sphere	Bi_2MoO_6	Self-aggregation combined with Ostwald ripening	176
	Sn-TiO_2	Ostwald ripening	178
	$\text{Fe}_3\text{O}_4-\text{ZnS}$	Corrosion-aided Ostwald ripening	179
Rattle-type hollow sphere	NiO-SnO_2	Ni template method	213
	$\text{TiO}_2@\text{void@SiO}_2$	LbL combined with photocatalytic method	192
	$\alpha\text{-Fe}_2\text{O}_3@\text{SnO}_2$	Inside-out Ostwald ripening	200
	$\text{Fe}_3\text{O}_4@\text{SiO}_2$	Carbon template method	208
Nanoparticles encapsulated in hollow sphere	$\text{SnO}_2@\text{carbon}$	Silica template method	86
	$\text{Sn}@\text{Carbon}$	Silica template method	199
	$\text{Pd}@\text{SiO}_2$	Carbon template method	76

or electrocatalytic properties. For example, Pt hollow nanospheres with an average diameter of 24 nm and discrete Pt nanoparticles, display twice the electrocatalytic activity of the solid Pt nanoclusters in the oxidation of methanol.¹¹¹ The hierarchical flower-like Bi_2MoO_6 hollow spheres exhibited excellent visible-light-driven photocatalytic efficiency for the degradation of Rhodamine B, up to 95% within 2 h, which was much higher than that of solid-state Bi_2MoO_6 and TiO_2 (P25).¹⁷⁶ By designing specific hollow structures, one can improve the catalytic property. For example, the rattle-structured hollow $\text{Au}@\text{ZrO}_2$ was used as a model high-temperature-stable catalyst for CO oxidation, in which the Au nanoparticles were effectively separated but still highly accessible to gas molecules.¹⁹¹ The rattle-type $\text{TiO}_2@\text{void@SiO}_2$ particles, with commercial TiO_2 particles encapsulated into hollow SiO_2 shells, showed high photocatalytic activity and UV-shielding performance without decomposing the supporting organic materials, as well as an increasing photocatalytic activity with an increasing thickness of void space.¹⁹²

In lithium-ion batteries, hollow nanomaterials made of Sn,^{193–195} and some transition metal oxides^{196,197} have recently been the focus of research into high-energy electrode materials

for novel lithium-ion batteries. Archer *et al.* used the SnO_2 hollow nanospheres as anode materials for lithium-ion batteries, demonstrating a surprisingly large initial discharge capacity of 1140 mA h g⁻¹, more than 75% greater than that of pristine SnO_2 nanoparticles (*ca.* 645 mA h g⁻¹).¹⁹⁸ Rattle-type structures with other functional cores in the interior void space exhibited excellent electrochemical properties in lithium storage capacities.¹⁹⁹ Uniform $\alpha\text{-Fe}_2\text{O}_3@\text{SnO}_2$ nanorattles with large void spaces were found to improve lithium storage capabilities. Their first discharge capacities were 1544 mA h g⁻¹, and corresponding charge capacities were 865 mA h g⁻¹.²⁰⁰ The same authors reported that complex hollow spheres assembled from anatase TiO_2 nanosheets with exposed (001) facets displayed the excellent cyclic retention even at high current rates.^{201,202}

Wang *et al.* used the complicated Co_3O_4 multishelled hollow spheres, including single shelled (S-Co), double shelled (D-Co) and triple shelled (T-Co) spheres composed of oriented self-assembled nanosheets as the anode material in lithium-ion batteries.²⁰³ These hollow microspheres exhibited excellent cycle performance and enhanced lithium storage capacity in contrast to the commercial Co_3O_4 as shown in Fig. 20. Double-shelled hollow structures in particular delivered an

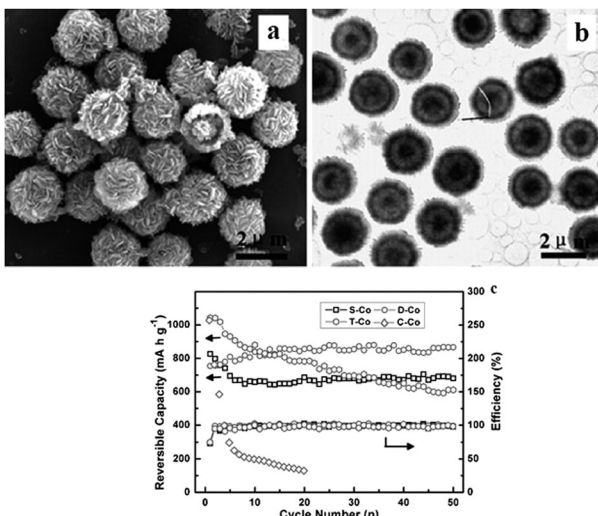


Fig. 20 SEM (a) and TEM (b) of the double shelled Co_3O_4 hollow spheres; (c) charge capacities *versus* cycle number and coulombic efficiency of the three as-prepared samples and commercial Co_3O_4 products (C-Co) at a current rate of $C/5$ (178 mA g^{-1}) between 3 V and 10 mV. Reprinted with permission from ref. 203. Copyright 2010 Wiley-VCH.

exceptional capacity of 866 mA H g^{-1} over 50 cycles at a current rate of $C/5$ (completing the charge or discharge process in 5 h; $1 \text{ C} = 890 \text{ mA g}^{-1}$).

In biomedical materials, the most important application of inorganic hollow spheres is drug loading and delivery.^{204–206} Magnetic and fluorescent hollow spheres are particularly preferred for this purpose.²⁰⁷ Combinations of mesoporous SiO_2 with magnetic particles to form magnetic mesoporous composites have great advantages for cancer therapy. SiO_2 hollow spheres with rattle-type magnetic cores and mesoporous shells not only enable high drug loading and magnetically targeted delivery but also facilitate drug molecules to diffuse into or out of the shells.²⁰⁸ Mesoporous and luminescence-functionalized $\text{CaF}_2:\text{Ce}^{3+}/\text{Tb}^{3+}$ hollow spheres have been used as drug carriers.²⁰⁹ Wu *et al.* reported that the $\text{Fe}_3\text{O}_4/\text{ZnS}$ hollow spheres synthesized *via* corrosion-aided Ostwald ripening, displayed not only superparamagnetism and fluorescence but also high drug loading capacity and a comparable release rate to conventional silica drug carriers, releasing more than 50 and 90% of the drug within 10 and 65 h, respectively.¹⁷⁹

Hollow spheres of semiconducting metal oxides can still find other uses such as gas sensing, because their large surface-to-volume ratios significantly enhance gas diffusion and mass transport in the sensing layers.^{210,211} For example, Au-studded porous SnO_2 hollow spheres could obviously improve sensor response. With ethanol, the responses to 10, 50, 100, 200, and 600 ppm were about 9.3, 21.2, 76.9, 129.8, and 147.8 times higher for Au-studded spheres than for SnO_2 hollow spheres alone. With acetone, the responses were about 5.8, 11.9, 24.5, 34.5, and 47.8 times higher than its original value.²¹² The ethanol sensors based on nanoscale SnO_2 hollow spheres with NiO-functionalized inner walls exhibited ultra-fast response and recovery. As shown in Fig. 21, the gas responses (R_a/R_g , R_a : resistance in air, R_g : resistance in gas) to 20, 50,

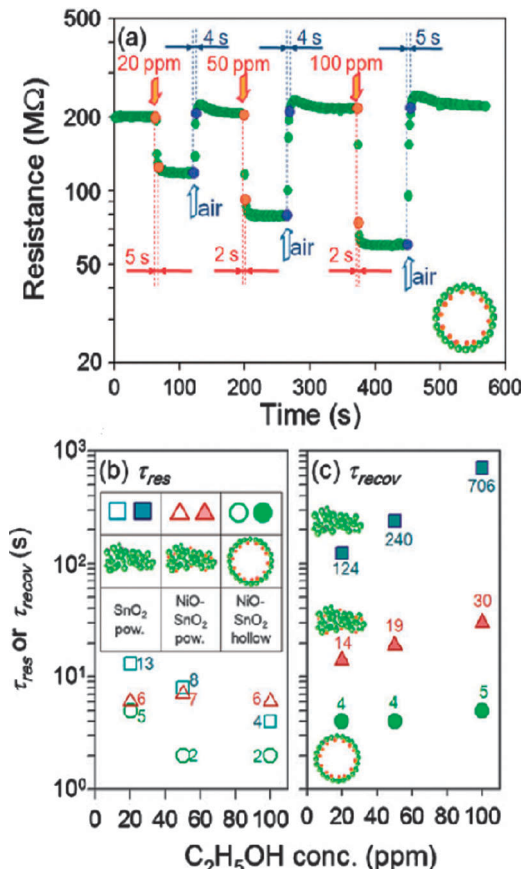


Fig. 21 (a) Dynamic $\text{C}_2\text{H}_5\text{OH}$ sensing transient of NiO-functionalized SnO_2 hollow spheres at 450 °C; (b–c) 90% responses and recovery times (τ_{res} and τ_{recov}) of the sensors. Reprinted with permission from ref. 213. Copyright 2010 Royal Society of Chemistry.

and 100 ppm ethanol were 1.75, 2.58, and 3.54, respectively. The times to reach 90% variation in resistance upon exposure to ethanol and air were defined as the 90% response time (τ_{res}) and the 90% recovery time (τ_{recov}), respectively. The τ_{res} values upon exposure to 20, 50, and 100 ppm ethanol were 5, 2, and 2 s, respectively. These fast responses and recovery characteristics can be attributed to rapid gas diffusion through the less agglomerated porous shells and the promotion of surface reaction by the NiO inner layers.²¹³

In addition, inorganic hollow spheres with large specific surface areas, such as those made from MgSiO_3 ,²¹⁴ Mn_2O_3 ,²¹⁵ and CeO_2 ²¹⁶ can be used as absorbents to remove organic molecules and heavy-metal ions from waste water. Recently, the interesting optical properties of hollow silica nanoparticles showed potential applications as optical devices. When particle size was adjusted from 333 to 642 nm, the color of powders created by resonant Mie scattering turned from blue to violet (Fig. 22).²¹⁷

5.2 Two-dimensional (2D) arrays

Another important potential application of inorganic hollow spheres is their 2D ordered structures. These arrays display special magnetic properties,²¹⁸ optical properties,²¹⁹ photocatalytic properties,²²⁰ gas sensing properties,²²¹ and surface-enhanced Raman scattering (SERS).²²² In this field, Cai and

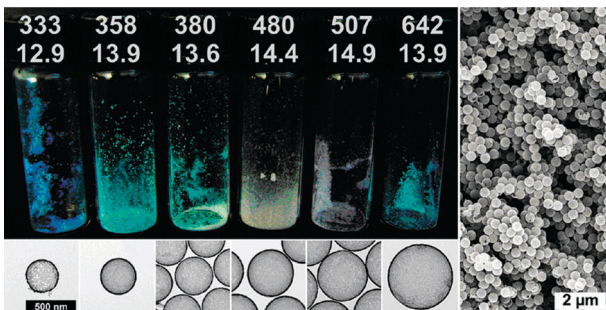


Fig. 22 Amorphous powders of hollow silica nanoparticles with increasing diameter from left to right. The numbers on top of the vials represent particle diameter and shell thickness in nanometres, respectively. Corresponding TEM images of individual particles are given in the bottom panel. SEM image of the 380 nm amorphous powder (right). Reprinted with permission from ref. 217. Copyright 2011 American Chemical Society.

his colleagues prepared a series of 2D arrays of inorganic hollow spheres from such substances as Si,²²³ CdS,²²⁴ NiO, Ni, and Ni(OH)²¹⁸ through deposition of hollow spheres onto conductive substrates combined with thermal treatment and subsequent solution-dipping, electrochemical deposition, or electrophoresis, and obtained some encouraging results. For example, the 2D array of Ni hollow spheres showed excellent magnetic properties.²²⁵ The coercivity values were 104 Oe for the applied field parallel to the film and 87 Oe for the applied field perpendicular to the film. These are larger than those of bulk Ni and hollow Ni submicrometer-sized spheres. The hierarchical Ni(OH)₂ monolayer hollow-sphere arrays also demonstrated a tunable optical transmission stop band in the visible-near-IR region from 455–1855 nm, depending on the size and fine structure of the hollow sphere (Fig. 23). Very interestingly, they unveiled a nearly incident-angle-independent position of the stop band, which 3D photonic crystals do not possess. This should be of great significance to applications in optical devices, photonic crystals, nanoscience, and nanotechnology.²²⁶

2D ordered hollow sphere arrays have also been shown to be good candidates for the SERS-active substrates due to the periodic characteristics and the nano-sized structures. The hierarchically micro/nanostructured rough Au particle arrays exhibited a strong SERS effect using Rhodamine 6G as probe molecules.²²² The SERS intensity at 1362 cm⁻¹ for the porous

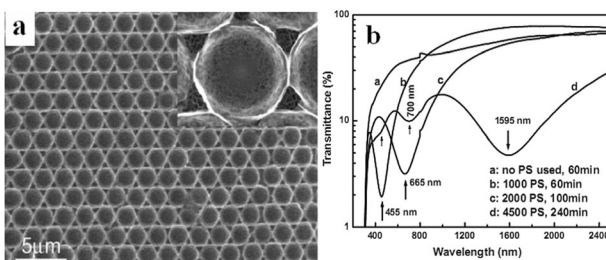


Fig. 23 (a) FE-SEM image of ordered Ni(OH)₂ arrays, (b) optical transmission spectra of Ni(OH)₂ arrays on indium tin oxide glass with the incident light perpendicular to the substrate. Reprinted with permission from ref. 226. Copyright 2007 Wiley-VCH.

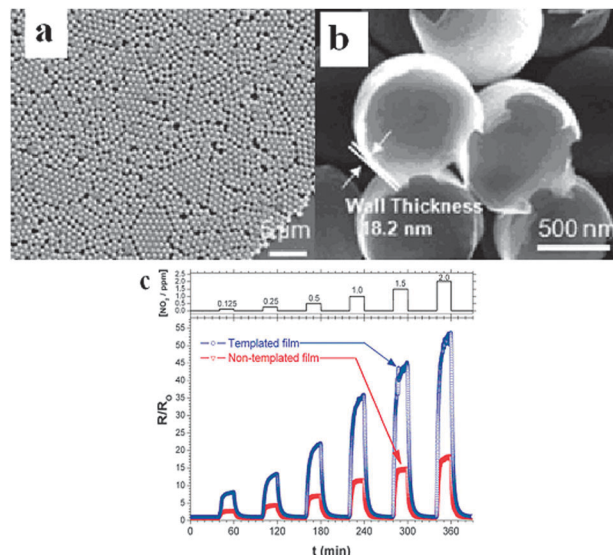


Fig. 24 (a-b) SEM images of hollow SnO₂ hemispheres; (c) The resistance response R/R_0 during cyclic exposure to increasing NO₂ concentration in dry air at 250 °C. The NO₂ gas concentration profile is shown on top. Reprinted with permission from ref. 227. Copyright 2009 Royal Society of Chemistry.

Au nanostructured film was about 2.5 times higher than that for the Au/Ag-coated silica film, and the SERS performance of such ordered porous nanostructured films could be stable for at least 3 months. Hollow SnO₂ hemisphere arrays (Fig. 24) fabricated *via* sputtering thin films of SnO₂ onto PMMA colloidal templates on alumina or Si substrates displayed a three-fold enhancement in sensitivity to NO₂ relative to non-templated counterparts. This ratio comes close to the geometric enhancement in their surface area (compared to flat films), which stands at 3.6 for an ideal 2D hexagonal close packed array of hemispheres.²²⁷

In addition, 2D structured porous films of SiO₂ hollow spheres on substrates prepared by a facile layer-by-layer dip-coating approach showed unique superhydrophilic and anti-fogging properties, attributable to both its surface roughness and surface porosity.²²⁸ The immediate water contact angle of this hollow sphere film was about 0°. The first water droplet spread flat in less than 0.033 s. When a control glass slide and a glass slide with superhydrophilic film after cooling at about -18 °C for 3 h were exposed to humid laboratory air (*ca.* 50% RH), the former glass fogged immediately and many dewdrops were observed on the glass surface. In contrast, the slide glass with the superhydrophilic film remained clear (Fig. 25).

5.3 Three-dimensional (3D) arrays

In addition to the above applications, inorganic hollow spheres can be self-assembled into 3D crystals, since 3D colloidal crystals have attracted great interest for their stability and potential applications in catalysis, anti-reflection coating, lithium ion batteries, and photonic materials such as optical filters, optical switches, and low-threshold lasers.^{229–232} For example, the 3D crystal film of TiO₂ hollow spheres exhibited higher photocatalytic activity compared to the

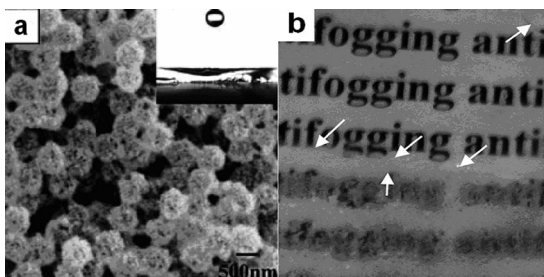


Fig. 25 (a) SEM image of the hierarchically structured porous film of silica hollow spheres (the inset shows the immediate water contact angle on the film); (b) antifogging properties of the slide glass coated with hollow sphere film (top), and of the uncoated slide glass (bottom). Reprinted with permission from ref. 228. Copyright 2008 Wiley-VCH.

reference TiO_2 flat film.²³³ The hollow SiO_2 nanoparticles were LbL-assembled on both PMMA and glass substrates to produce anti-reflection (AR) coatings. Single-index AR coatings can be made with optimized AR performance at any wavelength between 300 and 650 nm. In this case, reflection near the targeted wavelength was reduced from 7 to 0% and transmission was increased from 92 to 97% (Fig. 26).²³⁴ Although 3D-ordered hollow sphere arrays should be relevant to many applications, there are still many difficulties in controlling their size and morphology and preventing agglomeration.

Interestingly, close-packed-array photonic crystals (PCs) of SiO_2 shells were fabricated *via* the shrinkage of SiO_2 shell/poly(*N*-isopropylacrylamide) (PNIPAm) core particles during solvent evaporation and calcination for core removal. Compared to dry SiO_2 shell PCs, the Bragg diffraction peak wavelength of SiO_2 shell PCs in water only increased 5% in refractive index. This showed that these SiO_2 shells were impervious to water because the process of making them resulted in a continuous shell of silica without holes (Fig. 27).²³⁵

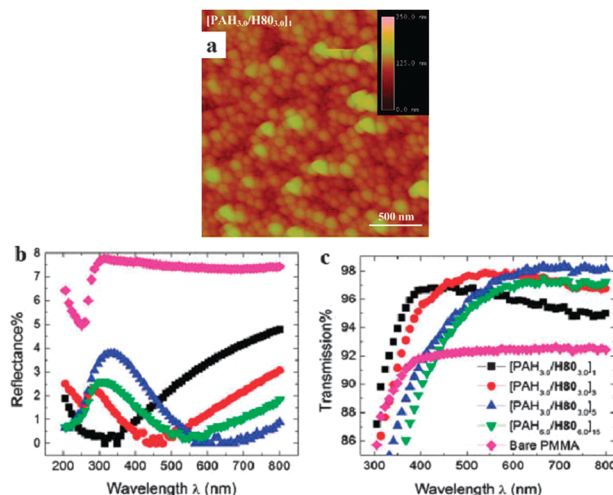


Fig. 26 (a) AFM of image of $\text{PAH}_{3.0}/\text{H}80_{3.01}$ on PMMA substrate, UV-VIS reflection (b) and transmission spectra (c) for the single index design on PMMA substrates. (PAH: poly(allylamine hydrochloride), H80: hollow SiO_2 nanoparticles). Reprinted with permission from ref. 234. Copyright 2010 American Chemical Society.

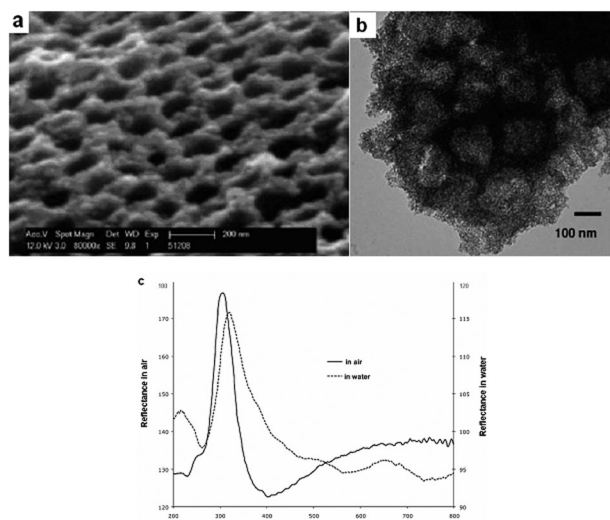


Fig. 27 (a) SEM images of the cross section of silica shell photonic crystals; (b) TEM image of the silica shell photonic crystals; (c) Reflectance spectra of silica shell photonic crystals in air and water. Reprinted with permission from ref. 235. Copyright 2009 American Chemical Society.

6. Summary and outlook

This review highlights the most important synthetic methods and applications of inorganic hollow spheres. The relative advances in the synthesis and properties of these particles have paved the way to a huge range of new materials with many potential applications. In this article, we have reported selected examples of inorganic hollow spheres prepared either using template strategies against (i) polymeric, (ii) inorganic nonmetallic, (iii) metallic particles, (iv) soft compounds, or from template-free strategies. We have also reported the potential applications of 0D, 2D, and 3D arrays.

Templating against polymeric colloids and inorganic nonmetallic particles such as silica and carbon is incontrovertibly the most efficient and common strategy of fabricating inorganic hollow spherical micro/nanomaterials. This is due to the controllable morphology and uniform size of the hollow spheres and theoretical universalism for various kinds of ceramic shells. Its complicated process is nonetheless unsatisfactory. In particular, removal of these templates by etching or calcination is not only time-consuming but can also cause collapse or deformation of the shell. Metallic template-based syntheses have been embraced by many researchers in recent years due to the lack of additional operating costs, such as functionalization and core template removal, but this technique is only used to prepare spheres from a few metals and metallic compounds.

The soft-template approach provides advantages such as easy template removal and efficient encapsulation of therapeutic and biologically active molecules. However, obtaining monodisperse size and spherical morphology is difficult because soft templates are usually thermodynamically unstable and can be influenced by factors such as the solvent polarity, pH value, and the ionic strength of the solution.

Template-free strategies such as the Ostwald ripening process can overcome the demerits of template strategies,

and obviously is becoming one of the most useful methods. However, this strategy is only useful for the synthesis of hollow spheres from certain special compounds.

Inorganic hollow spheres have many potential applications in catalysts, lithium-ion batteries, biomedical materials, gas sensors, mini-reactors, and other tools. Recent studies indicate that the 2D and 3D arrays of some inorganic hollow spheres have preferable and even novel characteristics.

Many fabrication methods and their related hollowing mechanisms have been proposed over the past ten years, but each approach has its pros and cons. This in turn provides us important research opportunities. In particular, we believe that the following aspects should be paid more attention in the future research and development of inorganic hollow spheres:

(i) As there is no single method that works well for every situation, the exploration of synergistic features and interconnections of two or more methods will be very interesting. It is foreseeable that one will be able to prepare the desired inorganic hollow spheres with controllable composition and properties and even more complex hollow architectures. In particular, researchers should explore universal, simple, and scalable methodologies for the fabrication of various commercial-scale, high-quality inorganic hollow spheres.

(ii) The Kirkendall effect and Ostwald ripening process can work very well under circumstances that confound polymer and nonmetal template approaches. However, these methods provide only certain prototypes. More comprehensive investigations should be carried out into the mechanism and process by which hollow spheres are formed *via* the Kirkendall effect and Ostwald ripening process. This may allow the community to expand the scope of these methods.

(iii) More practical applications may be envisioned by the integration of two or more performances, such as superparamagnetism, fluorescence, spectrum selectivity, biocompatibility, photocatalysis, mechanical properties, electrical properties, stimulus response, and dispersibility in media into hollow spheres through the assembly of different inorganic and organic components.

(iv) Although the properties and applications of inorganic hollow spheres themselves have been widely studied, the investigations themselves are relatively new. More importantly, the properties and potential applications of 2D and 3D arrays of inorganic hollow spheres are still new ground. New and even unprecedented properties should be expected for both fundamental research and applications. For example, 2D arrays of semiconducting hollow spheres are promising candidates for the key sensing of elements in optoelectronic devices due to their high area coverage ratios and large surface-to-volume ratios. 3D arrays of alternative inorganic hollow spheres and solid particles may enhance the bandwidth and reflectivity, which has great potential in reflective mirrors for microlasers.

We hope that the general preparation procedures and principles of each method, the selected samples reviewed in this article, and our personal opinions can provide readers with the necessary background and ideas to develop deeper expertise and more effective fabrication methods. We are confident that more versatile and powerful methods of

preparation of inorganic hollow spheres will be developed from both fundamental and practical viewpoints and that more novel physicochemical properties and applications will be explored in the near future.

Acknowledgements

The National Natural Science Foundation of China (No. 21074023), National “863” Foundation, Science and Technology Foundation of Shanghai (0952nm01000, 10JC1401900), the innovative team of the Ministry of Education of China (IRT0911), and Shanghai Chenguang Foundation (10CG60) are thanked for their financial support.

Notes and references

- Y. Zhu, J. Shi, W. Shen, X. Dong, J. Feng, M. Ruan and Y. Li, *Angew. Chem., Int. Ed.*, 2005, **44**, 5083.
- J. Yuan, K. Laubernds, Q. Zhang and S. L. Suib, *J. Am. Chem. Soc.*, 2003, **125**, 4966.
- Y. Zhu, Y. Fang and S. Kaskel, *J. Phys. Chem. C*, 2010, **114**, 16382.
- J. Liu, F. Liu, J. Wu and D. Xue, *J. Mater. Chem.*, 2009, **19**, 6073.
- A. Kowalski, M. Vogel and R. M. Blankenship, *US Patent* 4,427,836, 1884.
- R. M. Blankenship, *US Patent* 5,494,971, 1996.
- A. Imhof, *Langmuir*, 2001, **17**, 3579.
- C. E. Fowler, D. Khushalani and S. Mann, *Chem. Commun.*, 2001, 2028.
- R. K. Rana, Y. Mastai and A. Gedanken, *Adv. Mater.*, 2002, **14**, 1414.
- L. Song, X. Ge, M. Wang, Z. Zhang and S. Li, *J. Polym. Sci., Part A: Polym. Chem.*, 2006, **44**, 2533.
- C. Chen, S. F. Abbas, A. Morey, S. Sithambaram, L. Xu, H. F. Garces, W. A. Hines and S. L. Suib, *Adv. Mater.*, 2008, **20**, 1205.
- M. Zhao, L. Sun and R. M. Crooks, *J. Am. Chem. Soc.*, 1998, **120**, 4877.
- Q. Zhou, S. Wang, X. Fan, R. C. Advincula and J. Mays, *Langmuir*, 2002, **18**, 3324.
- C. Perruchot, M. A. Khan, A. Kamitsi, S. P. Armes and T. von Werne, *Langmuir*, 2001, **17**, 4479.
- T. von Werne and T. E. Patten, *J. Am. Chem. Soc.*, 2001, **123**, 7497.
- J. Wang, K. P. Loh, Y. Zhong, M. Lin, J. Ding and Y. Foo, *Chem. Mater.*, 2007, **19**, 2566.
- N. A. Dhas and K. S. Suslick, *J. Am. Chem. Soc.*, 2005, **127**, 2368.
- P. M. Arnal, C. Weidenthaler and F. Schüth, *Chem. Mater.*, 2006, **18**, 2733.
- R. Yang, H. Li, X. Qiu and L. Chen, *Chem.-Eur. J.*, 2006, **12**, 4083.
- I. D. Hosein and C. M. Liddell, *Langmuir*, 2007, **23**, 2892.
- J. Liu, A. I. Maaroof, L. Wieczorek and M. B. Cortie, *Adv. Mater.*, 2005, **17**, 1276.
- Y. Yin, Y. Lu, B. Gates and Y. Xia, *Chem. Mater.*, 2001, **13**, 1146.
- Z. Liang, A. Susha and F. Caruso, *Chem. Mater.*, 2003, **15**, 3176.
- R. H. A. Ras, M. Kemell, J. D. Wit, M. Ritala, G. T. Brinke, M. Leskelä and O. Ikkala, *Adv. Mater.*, 2007, **19**, 102.
- S. J. Kim, C. S. Ah and D. Jang, *Adv. Mater.*, 2007, **19**, 1064.
- H. Zhou, T. Fan, D. Zhang, Q. Guo and H. Ogawa, *Chem. Mater.*, 2007, **19**, 2144.
- D. Yang, S. Chen, P. Huang, X. Wang, W. Jiang, O. Pandoli and D. Cui, *Green Chem.*, 2010, **12**, 2038.
- J. Huang, Y. Xie, B. Li, Y. Liu, Y. Qian and S. Zhang, *Adv. Mater.*, 2000, **12**, 808.
- S. Wang, F. Gu and M. K. Lü, *Langmuir*, 2006, **22**, 398.
- G. Chen, D. Xia, Z. Nie, Z. Wang, L. Wang, L. Zhang and J. Zhang, *Chem. Mater.*, 2007, **19**, 1840.
- G. Réthoré and A. Pandit, *Small*, 2010, **6**, 488.
- X. Lou, L. A. Archer and Z. Yang, *Adv. Mater.*, 2008, **20**, 3987.

- 33 Y. Zhao and L. Jiang, *Adv. Mater.*, 2009, **21**, 3621.
- 34 H. Zeng, *J. Mater. Chem.*, 2011, **21**, 7511, DOI: 10.1039/cljm10499c.
- 35 Z. Yang, H. Cong and W. Cao, *J. Polym. Sci., Part A: Polym. Chem.*, 2004, **42**, 4284.
- 36 Z. Zhong, Y. Yin, B. Gates and Y. Xia, *Adv. Mater.*, 2000, **12**, 206.
- 37 H. Yoshikawa, K. Hayasida, Y. Kozuka, A. Horiguchi, K. Awaga, S. Bandow and S. Iijima, *Appl. Phys. Lett.*, 2004, **85**, 5287.
- 38 M. Ohnishi, Y. Kozuka, Q. Ye, H. Yoshikawa, K. Awaga, R. Matsuno, M. Kobayashi, A. Takahara, T. Yokoyama, S. Bandow and S. Iijima, *J. Mater. Chem.*, 2006, **16**, 3215.
- 39 X. Chen, W. Yang, S. Wang, M. Qiao, S. Yan, K. Fan and H. He, *New J. Chem.*, 2005, **29**, 266.
- 40 D. Wang, C. Song, Z. Hu and X. Fu, *J. Phys. Chem. B*, 2005, **109**, 1125.
- 41 M. Agrawal, A. Pich, S. Gupta, N. E. Zafeiropoulos, P. Simon and M. Stamm, *Langmuir*, 2008, **24**, 1013.
- 42 I. Yamaguchi, M. Watanabe, T. Shinagawa, M. Chigane, M. Inaba, A. Tasaka and M. Izaki, *ACS Appl. Mater. Interfaces*, 2009, **1**, 1070.
- 43 I. Tissot, J. P. Reymond, F. Lefebvre and E. Bourgeat-lami, *Chem. Mater.*, 2002, **14**, 1325.
- 44 Z. Yang, Z. Niu, Y. Lu, Z. Hu and C. C. Han, *Angew. Chem., Int. Ed.*, 2003, **42**, 1943.
- 45 M. Yang, J. Ma, C. Zhang, Z. Yang and Y. Lu, *Angew. Chem., Int. Ed.*, 2005, **44**, 6727.
- 46 M. Yang, J. Ma, Z. Niu, X. Dong, H. Xu, Z. Meng, Z. Jin, Y. Lu, Z. Hu and Z. Yang, *Adv. Funct. Mater.*, 2005, **15**, 1523.
- 47 M. Yang, J. Ma, S. Ding, Z. Meng, J. Liu, T. Zhao, L. Mao, Y. Shi, X. Jin, Y. Lu and Z. Yang, *Macromol. Chem. Phys.*, 2006, **207**, 1633.
- 48 H. Xu, W. Wei, C. Zhang, S. Ding, X. Qu, J. Liu, Y. Lu and Z. Yang, *Chem.-Asian J.*, 2007, **2**, 828.
- 49 Y. Zeng, X. Wang, H. Wang, Y. Dong, Y. Ma and J. Yao, *Chem. Commun.*, 2010, **46**, 4312.
- 50 G. Jia, H. You, Y. Zheng, K. Liu, N. Guo and H. Zhang, *CrystEngComm*, 2010, **12**, 2943.
- 51 R. A. Caruso, A. Susha and F. Caruso, *Chem. Mater.*, 2001, **13**, 400.
- 52 F. Caruso, R. A. Caruso and H. Möhwald, *Science*, 1998, **282**, 1111.
- 53 F. Caruso, X. Shi, R. A. Caruso and A. Susha, *Adv. Mater.*, 2001, **13**, 740.
- 54 L. Wang, Y. Ebina, K. Takada and T. Sasaki, *Chem. Commun.*, 2004, 1074.
- 55 X. Wang, W. Yang, Y. Tang, Y. Wang, S. Fu and Z. Gao, *Chem. Commun.*, 2000, 2161.
- 56 F. Caruso, M. Spasova, A. Susha, M. Giersig and R. A. Caruso, *Chem. Mater.*, 2001, **13**, 109.
- 57 M. Chen, L. Wu, S. Zhou and B. You, *Adv. Mater.*, 2006, **18**, 801.
- 58 X. Cheng, M. Chen, L. Wu and B. You, *J. Polym. Sci., Part A: Polym. Chem.*, 2007, **45**, 3431.
- 59 X. Cheng, M. Chen, L. Wu and G. Gu, *Langmuir*, 2006, **22**, 3858.
- 60 Z. Deng, M. Chen, S. Zhou, B. You and L. Wu, *Langmuir*, 2006, **22**, 6403.
- 61 Z. Deng, M. Chen, G. Gu and L. Wu, *J. Phys. Chem. B*, 2008, **112**, 16.
- 62 Z. Wang, M. Chen and L. Wu, *Langmuir*, 2009, **25**, 7646.
- 63 W. Leng, M. Chen, S. Zhou and L. Wu, *Langmuir*, 2010, **26**, 14271.
- 64 M. Chen, L. Xie, S. Zhou, F. Li and L. Wu, *ACS Appl. Mater. Interfaces*, 2010, **2**, 2738.
- 65 H. Liu, Y. Wang, K. Wang, E. Hosono and H. Zhou, *J. Mater. Chem.*, 2009, **19**, 2835.
- 66 N. Wang, Y. Gao, J. Gong, X. Ma, X. Zhang, Y. Guo and L. Qu, *Eur. J. Inorg. Chem.*, 2008, 3827.
- 67 H. Qian, G. Lin, Y. Zhang, P. Gunawan and R. Xu, *Nanotechnology*, 2007, **18**, 11.
- 68 Y. Liu, P. Yang, W. Wang, H. Donga and J. Lin, *CrystEngComm*, 2010, **12**, 3717.
- 69 X. Sun and Y. Li, *Angew. Chem., Int. Ed.*, 2004, **43**, 597.
- 70 X. Sun and Y. Li, *Angew. Chem., Int. Ed.*, 2004, **43**, 3827.
- 71 X. Sun, J. Liu and Y. Li, *Chem.-Eur. J.*, 2006, **12**, 2039.
- 72 J. H. Bang and K. S. Suslick, *J. Am. Chem. Soc.*, 2007, **129**, 2242.
- 73 M. Titirici, M. Antonietti and A. Thomas, *Chem. Mater.*, 2006, **18**, 3808.
- 74 Y. Meng, D. Cheng and X. Jiao, *Eur. J. Inorg. Chem.*, 2008, 4019.
- 75 Y. Xia and R. Mokaya, *J. Mater. Chem.*, 2005, **15**, 3126.
- 76 Z. Chen, Z. Cui, F. Niu, L. Jiang and W. Song, *Chem. Commun.*, 2010, **46**, 6524.
- 77 Y. Zhang, E. Shi, Z. Chen, X. Li and B. Xiao, *J. Mater. Chem.*, 2006, **16**, 4141.
- 78 J. Wang, Y. Zhu, Y. Wu, C. Wu, D. Xu and Z. Zhang, *Mod. Phys. Lett. B*, 2006, **20**, 549.
- 79 P. Jin, Q. W. Chen, L. Q. Hao, R. F. Tian, L. X. Zhang and L. Wang, *J. Phys. Chem. B*, 2004, **108**, 6311.
- 80 J. Feng and Q. Wang, *J. Am. Ceram. Soc.*, 2009, **92**, 235.
- 81 Y. Piao, K. An, J. Kim, T. Yu and T. Hyeon, *J. Mater. Chem.*, 2006, **16**, 2984.
- 82 S. W. Kim, M. Kim, W. Y. Lee and T. Hyeon, *J. Am. Chem. Soc.*, 2002, **124**, 7642.
- 83 F. Su, X. Zhao, Y. Wang, L. Wang and J. Y. Lee, *J. Mater. Chem.*, 2006, **16**, 4413.
- 84 Y. Wang, G. Wang, H. Wang, W. Cai and L. Zhang, *Chem. Commun.*, 2008, 6555.
- 85 Y. Wang, C. Tang, Q. Deng, C. Liang, D. H. L. Ng, F. L. Kwong, H. Wang, W. Cai, L. Zhang and G. Wang, *Langmuir*, 2010, **26**, 14830.
- 86 W. Zhang, J. Hu, Y. Guo, S. Zheng, L. Zhong, W. Song and L. Wan, *Adv. Mater.*, 2008, **20**, 1160.
- 87 H. A. Esfahani, Y. Nemoto, L. Wang and Y. Yamauchi, *Chem. Commun.*, 2011, **47**, 3885.
- 88 F. Piret, C. Bouvy and B. L. Su, *J. Mater. Chem.*, 2009, **19**, 5964.
- 89 Z. Wang, Y. Liu, J. G. Jiang, M. He and P. Wu, *J. Mater. Chem.*, 2010, **20**, 10193.
- 90 K. Wang, H. Wang and Y. B. Cheng, *Chem. Commun.*, 2010, **46**, 303.
- 91 A. D. Smigelskas and E. O. Kirkendall, *Trans. Am. Inst. Min. Metall. Pet. Eng.*, 1947, **171**, 130.
- 92 J. Gao, B. Zhang, X. Zhang and B. Xu, *Angew. Chem.*, 2006, **118**, 1242.
- 93 Y. Yin, R. M. Rioux, C. K. Erdonmez, S. Hughes, G. A. Somorjai and A. P. Alivisatos, *Science*, 2004, **304**, 711.
- 94 Y. Yin, C. K. Erdonmez, A. Cabot, S. Hughes and A. P. Alivisatos, *Adv. Funct. Mater.*, 2006, **16**, 1389.
- 95 Z. Shan, G. Adesso, A. Cabot, M. P. Sherburne, S. A. Syed Asif, O. L. Warren, D. C. Chrzan, A. M. Minor and A. P. Alivisatos, *Nat. Mater.*, 2008, **7**, 947.
- 96 A. Cabot, A. P. Alivisatos, V. F. Puntes, L. balcells, Ó. Iglesias and A. Labarta, *Phys. Rev. B*, 2009, **79**, 094419.
- 97 A. Cabot, M. Ibáñez, P. Guardia and A. P. Alivisatos, *J. Am. Chem. Soc.*, 2009, **131**, 11326.
- 98 J. Gao, B. Zhang, X. Zhang and B. Xu, *Angew. Chem., Int. Ed.*, 2006, **45**, 1220.
- 99 J. Gao, G. Liang, B. Zhang, Y. Kuang, X. Zhang and B. Xu, *J. Am. Chem. Soc.*, 2007, **129**, 1428.
- 100 R. K. Chiang and R. T. Chiang, *Inorg. Chem.*, 2007, **46**, 369.
- 101 A. E. Henkes, Y. Vasquez and R. E. Schaak, *J. Am. Chem. Soc.*, 2007, **129**, 1896.
- 102 C. M. Wang, D. R. Baer, L. E. Thomas, J. E. Amonette, J. Antony, Y. Qiang and G. Duscher, *J. Appl. Phys.*, 2005, **98**, 094308.
- 103 A. H. Latham, M. J. Wilson, P. Schiffer and M. E. Williams, *J. Am. Chem. Soc.*, 2006, **128**, 12632.
- 104 D. Farrell, S. A. Majetich and J. P. Wilcoxon, *J. Phys. Chem. B*, 2003, **107**, 11022.
- 105 S. Peng and S. Sun, *Angew. Chem., Int. Ed.*, 2007, **46**, 4155.
- 106 K. An, S. G. Kwon, M. Park, H. B. Na, S. I. Baik, J. H. Yu, D. Kim, J. S. Son, Y. W. Kim, I. C. Song, W. K. Moon, H. M. Park and T. Hyeon, *Nano Lett.*, 2008, **12**, 4252.
- 107 J. Park, H. Zheng, Y. W. Jun and A. P. Alivisatos, *J. Am. Chem. Soc.*, 2009, **131**, 13943.
- 108 Y. Sun, B. T. Mayers and Y. Xia, *Nano Lett.*, 2002, **5**, 481.
- 109 Y. Sun, B. Mayers and Y. Xia, *Adv. Mater.*, 2003, **15**, 641.
- 110 M. Chen and L. Gao, *Inorg. Chem.*, 2006, **45**, 5145.
- 111 H. Liang, H. Zhang, J. Hu, Y. Guo, L. Wan and C. Bai, *Angew. Chem.*, 2004, **116**, 1566.
- 112 H. Liang, L. Wan, C. Bai and L. Jiang, *J. Phys. Chem. B*, 2005, **109**, 7795.
- 113 H. Liang, Y. Guo, H. Zhang, J. Hu, L. Wan and C. Bai, *Chem. Commun.*, 2004, 1496.
- 114 S. Guo, S. Dong and E. Wang, *Chem.-Eur. J.*, 2008, **14**, 4689.

- 115 Q. Sun, Z. Ren, R. Wang, N. Wang and X. Cao, *J. Mater. Chem.*, 2011, **21**, 1925.
- 116 J. Bao, Y. Liang, Z. Xu and L. Si, *Adv. Mater.*, 2003, **15**, 1832.
- 117 C. E. Fowler, D. Khushalani and S. Mann, *J. Mater. Chem.*, 2001, **11**, 1968.
- 118 T. Nakashima and N. Kimizuka, *J. Am. Chem. Soc.*, 2003, **125**, 6386.
- 119 B. Peng, M. Chen, S. Zhou, L. Wu and X. Ma, *J. Colloid Interface Sci.*, 2008, **321**, 67.
- 120 B. P. Bastakoti, S. Guragain, Y. Yokoyama, S. Yusa and K. Nakashima, *Langmuir*, 2011, **27**, 379.
- 121 C. I. Zoldesi and A. Imhof, *Adv. Mater.*, 2005, **17**, 924.
- 122 C. I. Zoldesi, C. A. van Walree and A. Imhof, *Langmuir*, 2006, **22**, 4343.
- 123 P. Leidinger, R. Popescu, D. Gerthsen and C. Feldmann, *Small*, 2010, **6**, 1886.
- 124 C. Kind, R. Popescu, E. Müller, D. Gerthsen and C. Feldmann, *Nanoscale*, 2010, **2**, 2223.
- 125 L. Li, E. S. Choo, X. Tang, J. Ding and J. Xue, *Chem. Commun.*, 2009, 938.
- 126 Z. Wang, M. Chen and L. Wu, *Chem. Mater.*, 2008, **20**, 3251.
- 127 Y. Zhao, J. Zhang, W. Li, C. Zhang and B. Han, *Chem. Commun.*, 2009, 2365.
- 128 J. Wang, Y. Xia, W. Wang, M. Poliakoff and R. Mokaya, *J. Mater. Chem.*, 2006, **16**, 1751.
- 129 Q. Sun, P. C. M. M. Magusin, B. Mezari, P. Panine, R. A. van Santen and N. A. J. M. Sommerdijk, *J. Mater. Chem.*, 2005, **15**, 256.
- 130 Y. Chen, Y. Li, Y. Chen, X. Liu, M. Zhang, B. Li and Y. Yang, *Chem. Commun.*, 2009, 5177.
- 131 H. Cong and S. Yu, *Adv. Funct. Mater.*, 2007, **17**, 1814.
- 132 X. Yu, C. Cao, H. Zhu, Q. Li, C. Liu and Q. Gong, *Adv. Funct. Mater.*, 2007, **17**, 1397.
- 133 H. Lin, C. Mou, S. B. Liu and C. Tang, *Chem. Commun.*, 2001, 1970.
- 134 H. Xu and W. Wang, *Angew. Chem., Int. Ed.*, 2007, **46**, 1489.
- 135 W. Wang, X. Tu, P. Zhang and G. Zhang, *CrystEngComm*, 2011, **13**, 1838.
- 136 C. Cao, Y. Gao, L. Kang and H. Luo, *CrystEngComm*, 2010, **12**, 4048.
- 137 G. Zhou, M. Lu, Z. Xiu, S. Wang, H. Zhang and W. Zou, *J. Cryst. Growth*, 2005, **276**, 116.
- 138 J. Zhou, J. Shi, W. Shen, H. Chen, X. Dong and M. Ruan, *Nanotechnology*, 2005, **16**, 2633.
- 139 G. Xi, Y. Peng, L. Xu, M. Zhang, W. Yu and Y. Qian, *Inorg. Chem. Commun.*, 2004, **7**, 607.
- 140 J. Guan, F. Mou, Z. Sun and W. Shi, *Chem. Commun.*, 2010, **46**, 6605.
- 141 L. Han, P. Xiong, J. Bai and S. Che, *J. Am. Chem. Soc.*, 2011, **133**, 6106.
- 142 J. Liu, S. B. Hartono, Y. Jin, Z. Li, G. Lu and S. Qiao, *J. Mater. Chem.*, 2010, **20**, 4595.
- 143 L. Guo, F. Liang, X. Wen, S. Yang, L. He, W. Zheng, C. Chen and Q. Zhong, *Adv. Funct. Mater.*, 2007, **17**, 425.
- 144 H. Hou, Q. Peng, S. Zhang, Q. Guo and Y. Xie, *Eur. J. Inorg. Chem.*, 2005, 2625.
- 145 W. Wang, P. Zhang, L. Peng, W. Xie, G. Zhang, Y. Tu and W. Mai, *CrystEngComm*, 2010, **12**, 700.
- 146 J. Wang, Y. Xia, W. Wang, R. Mokaya and M. Poliakoff, *Chem. Commun.*, 2005, 210.
- 147 W. Ostwald, *Z. Phys. Chem.*, 1900, **34**, 495.
- 148 X. Yan, D. Xu and D. Xue, *Acta Mater.*, 2007, **55**, 5747.
- 149 D. Xu and D. Xue, *J. Cryst. Growth*, 2006, **286**, 108.
- 150 L. Zhu, H. Xiao, W. Zhang, G. Yang and S. Fu, *Cryst. Growth Des.*, 2008, **8**, 957.
- 151 W. Cheng, K. Tang, Y. Qi, J. Sheng and Z. Liu, *J. Mater. Chem.*, 2010, **20**, 1799.
- 152 X. Wang, F. Yuan, P. Hu, L. Yu and L. Bai, *J. Phys. Chem. C*, 2008, **112**, 8773.
- 153 X. Cao, L. Gu, L. Zhuge, W. J. Gao, W. Wang and S. Wu, *Adv. Funct. Mater.*, 2006, **16**, 896.
- 154 X. Dai, Y. Luo, W. Zhang and S. Fu, *Dalton Trans.*, 2010, **39**, 3426.
- 155 C. Guo, Y. Cao, S. Xie, W. Dai and K. N. Fan, *Chem. Commun.*, 2003, 700.
- 156 J. Li and H. Zeng, *Angew. Chem., Int. Ed.*, 2005, **44**, 4342.
- 157 H. Yang and H. Zeng, *Angew. Chem., Int. Ed.*, 2004, **43**, 5206.
- 158 H. Li, Z. F. Bian, J. Zhu, D. Zhang, G. Li, Y. Huo, H. Li and Y. Lu, *J. Am. Chem. Soc.*, 2007, **129**, 8406.
- 159 Y. Xie, J. Huang, B. Li, Y. Liu and Y. Qian, *Adv. Mater.*, 2000, **12**, 1523.
- 160 C. Wang, K. Tang and Q. Yang, *J. Mater. Chem.*, 2002, **12**, 2426.
- 161 Y. Zhu, D. Fan and W. Shen, *J. Phys. Chem. C*, 2007, **111**, 18629.
- 162 L. Li, Y. Chu, Y. Liu and L. Dong, *J. Phys. Chem. C*, 2007, **111**, 2123.
- 163 H. Yang and H. Zeng, *J. Phys. Chem. B*, 2004, **108**, 3492.
- 164 Y. Chang, J. J. Teo and H. Zeng, *Langmuir*, 2005, **21**, 1074.
- 165 Y. Wang, Q. Zhu and H. Zhang, *Chem. Commun.*, 2005, 5231.
- 166 Y. Wang, Q. Zhu and H. Zhang, *J. Mater. Chem.*, 2006, **16**, 1212.
- 167 Z. Shen, J. Wang, P. Sun, D. Ding and T. Chen, *Chem. Commun.*, 2009, 1742.
- 168 X. Yu, J. Yu, B. Cheng and B. Huang, *Chem.-Eur. J.*, 2009, **15**, 6731.
- 169 J. Yu, H. Guo, S. A. Davis and S. Mann, *Adv. Funct. Mater.*, 2006, **16**, 2035.
- 170 H. Yu, J. Yu, S. Liu and S. Mann, *Chem. Mater.*, 2007, **19**, 4327.
- 171 J. Yu, H. Yu, H. Guo, M. Li and S. Mann, *Small*, 2008, **4**, 87.
- 172 J. Yu and J. Zhang, *Dalton Trans.*, 2010, **39**, 5860.
- 173 Z. An, J. Zhang and S. Pan, *Dalton Trans.*, 2009, 3664.
- 174 Z. An, S. Pan, J. Zhang and G. Song, *Dalton Trans.*, 2008, 5155.
- 175 P. Tartaj, T. Gonzalez-Carreño and C. J. Serna, *Adv. Mater.*, 2001, **13**, 1620.
- 176 G. Tian, Y. Chen, W. Zhou, K. Pan, Y. Dong, C. Tian and H. Fu, *J. Mater. Chem.*, 2011, **21**, 887.
- 177 B. Liu and H. Zeng, *Small*, 2005, **1**, 566.
- 178 J. Li and H. Zeng, *J. Am. Chem. Soc.*, 2007, **129**, 15839.
- 179 Z. Wang, L. Wu, M. Chen and S. Zhou, *J. Am. Chem. Soc.*, 2009, **131**, 11276.
- 180 D. Wheeler, R. Newhouse, H. Wang, S. Zou and J. Z. Zhang, *J. Phys. Chem. C*, 2010, **114**, 18126.
- 181 J. Z. Zhang, *J. Phys. Chem. Lett.*, 2010, **1**, 686.
- 182 S. Ikeda, S. Ishino, T. Harada, N. Okamoto, T. Sakata, H. Mori, S. Kuwabata, T. Torimoto and M. Matsumura, *Angew. Chem., Int. Ed.*, 2006, **45**, 7063.
- 183 H. Li, Z. Zhu, H. Li, P. Li and X. Zhou, *J. Colloid Interface Sci.*, 2010, **349**, 613.
- 184 Y. Li, P. Zhou, Z. Dai, Z. Hu, P. Sun and J. Bao, *New J. Chem.*, 2006, **30**, 832.
- 185 T. Harada, S. Ikeda, F. Hashimoto, T. Sakata, K. Ikeue, T. Torimoto and M. Matsumura, *Langmuir*, 2010, **26**, 17720.
- 186 D. Chen and J. Ye, *Adv. Funct. Mater.*, 2008, **18**, 1922.
- 187 J. Yu and L. Shi, *J. Mol. Catal. A: Chem.*, 2010, **326**, 8.
- 188 S. Liu, J. Yu and M. Jaroniec, *J. Am. Chem. Soc.*, 2008, **130**, 15808.
- 189 W. Wang, Y. Zhu and L. Yang, *Adv. Funct. Mater.*, 2007, **17**, 59.
- 190 D. G. Shchukin and R. A. Caruso, *Chem. Mater.*, 2004, **16**, 2287.
- 191 P. M. Arnal, M. Comotti and F. Schüth, *Angew. Chem., Int. Ed.*, 2006, **45**, 8224.
- 192 Y. Ren, M. Chen, Y. Zhang and L. Wu, *Langmuir*, 2010, **26**, 11391.
- 193 K. T. Lee, Y. S. Jung and S. M. Oh, *J. Am. Chem. Soc.*, 2003, **125**, 5652.
- 194 Y. Wang, F. Su, J. Y. Lee and X. S. Zhao, *Chem. Mater.*, 2006, **18**, 1347.
- 195 S. Han, B. Jang, T. Kim, S. M. Oh and T. Hyeon, *Adv. Funct. Mater.*, 2005, **15**, 1845.
- 196 A. Cao, J. Hu, H. Liang and L. Wan, *Angew. Chem., Int. Ed.*, 2005, **44**, 4391.
- 197 L. Jin, L. Xu, C. Morein, C. Chen, M. Lai, S. Dharmaratha, A. Dobley and S. L. Suib, *Adv. Funct. Mater.*, 2010, **20**, 3373.
- 198 X. Lou, Y. Wang, C. Yuan, J. Y. Lee and L. A. Archer, *Adv. Mater.*, 2006, **18**, 2325.
- 199 X. Wang, J. Hu, Y. Guo, S. Zheng, L. Zhong, W. Song and L. Wan, *Adv. Mater.*, 2008, **20**, 1160.
- 200 J. Chen, C. Li, W. Zhou, Q. Yan, L. A. Archer and X. Lou, *Nanoscale*, 2009, **1**, 280.
- 201 J. Chen, D. Luan, C. Li, F. Y. C. Boey, S. Qiao and X. Lou, *Chem. Commun.*, 2010, **46**, 8252.
- 202 S. Ding, J. S. Chen, Z. Wang, Y. L. Xheah, S. Madhavi, X. Hu and X. Lou, *J. Mater. Chem.*, 2011, **21**, 1677.

- 203 X. Wang, X. Wu, Y. Guo, Y. Zhong, X. Cao, Y. Ma and J. Yao, *Adv. Funct. Mater.*, 2010, **20**, 1680.
- 204 J. Zhou, W. Wu, D. Caruntu, M. Yu, A. Martin, J. Chen, C. J. O'Connor and W. Lou, *J. Phys. Chem. C*, 2007, **111**, 17473.
- 205 X. Jiang, T. L. Ward, Y. S. Cheng, J. Liu and C. J. Brinker, *Chem. Commun.*, 2010, **46**, 3019.
- 206 W. Wei, G. Ma, G. Hu, D. Yu, T. Mcleish, Z. Su and Z. Shen, *J. Am. Chem. Soc.*, 2008, **130**, 15808.
- 207 J. Shin, R. M. Anisur, M. K. Ko, G. H. Im, J. H. Lee and I. S. Lee, *Angew. Chem., Int. Ed.*, 2009, **48**, 321.
- 208 Y. Zhu, T. Ikoma, N. Hanagata and S. Kaskel, *Small*, 2010, **6**, 471.
- 209 C. Zhang, C. Li, C. Peng, R. Chai, S. Huang, D. Yang, Z. Cheng and J. Lin, *Chem. Eur. J.*, 2010, **16**, 5672.
- 210 X. Li, T. Lou, X. Sun and Y. Li, *Inorg. Chem.*, 2004, **43**, 5442.
- 211 F. Gyger, M. Hübner, C. Feldmann, N. Barsan and U. Weimar, *Chem. Mater.*, 2010, **22**, 4821.
- 212 J. Zhang, X. Liu, S. Wu, M. Xu, X. Guo and S. Wang, *J. Mater. Chem.*, 2010, **20**, 6453.
- 213 H. R. Kim, K. I. Choi, K. M. Kim, I. D. Kim, G. Cao and J. H. Lee, *Chem. Commun.*, 2010, **46**, 5061.
- 214 Y. Wang, G. Wang, H. Wang, C. Liang, W. Cai and L. Zhang, *Chem.-Eur. J.*, 2010, **16**, 3497.
- 215 J. Cao, Y. Zhu, L. Shi, L. Zhu, K. Bao, S. Liu and Y. Qian, *Eur. J. Inorg. Chem.*, 2010, 1172.
- 216 Z. Yang, J. Wei, H. Yang, L. Liu, H. Liang and Y. Yang, *Eur. J. Inorg. Chem.*, 2010, 3354.
- 217 M. Retsch, M. Schmelzeisen, H. J. Butt and E. L. Thomas, *Nano Lett.*, 2011, **11**, 1389.
- 218 G. Duan, W. Cai, Y. Luo, Z. Li and Y. Lei, *J. Phys. Chem. B*, 2006, **110**, 15729.
- 219 J. Elias, C. Lévy-Clément, M. Bechelany, J. Michler, G. Wang, Z. Wang and L. Philippe, *Adv. Mater.*, 2010, **22**, 1607.
- 220 H. Strohm and P. Löbmann, *J. Mater. Chem.*, 2004, **14**, 2667.
- 221 H. G. Moon, Y. S. Shim, H. W. Choi, C. Y. Kang, J. W. Choi, H. H. Park and S. J. Yoon, *Sens. Actuators, B*, 2010, **149**, 116.
- 222 L. Lu, A. Eychmüller, A. Kobayashi, Y. Hirano, K. Yoshida, Y. Kikkawa, K. Tawa and Y. Ozaki, *Langmuir*, 2006, **22**, 2605.
- 223 S. Yang, W. Cai, J. Yang and H. Zeng, *Langmuir*, 2009, **25**, 8287.
- 224 G. Duan, F. Lv, W. Cai, Y. Luo, Y. Li and G. Liu, *Langmuir*, 2010, **26**, 6295.
- 225 G. Duan, W. Cai, Y. Li, Z. Li, B. Cao and Y. Luo, *J. Phys. Chem. B*, 2006, **110**, 7184.
- 226 G. Duan, W. Cai, Y. Luo and F. Sun, *Adv. Funct. Mater.*, 2007, **17**, 644.
- 227 Y. E. Chang, D. Y. Youn, G. Ankonina, D. J. Yang, H. G. Kim, A. Rothschild and I. D. Kim, *Chem. Commun.*, 2009, 4019.
- 228 X. Liu, X. Du and J. He, *ChemPhysChem*, 2008, **9**, 305.
- 229 H. Wang, J. S. Yu, X. Li and D. P. Kim, *Chem. Commun.*, 2004, 2352.
- 230 L. Fu, T. Zhang, Q. Cao, H. Zhang and Y. Wu, *Electrochem. Commun.*, 2007, **9**, 2140.
- 231 E. M. Mitsuishi, J. Matsuiab and T. Miyashita, *J. Mater. Chem.*, 2009, **19**, 325.
- 232 M. C. Y. Huang, Y. Zhou and C. J. Chang-Hasnain, *Nat. Photonics*, 2007, **1**, 119.
- 233 Y. Li, T. Kunitake and S. Fujikawa, *J. Phys. Chem. B*, 2006, **110**, 13000.
- 234 Y. Du, L. E. Luna, W. S. Tan, M. F. Rubner and R. E. Cohen, *ACS Nano*, 2010, **4**, 4308.
- 235 L. Wang and S. A. Asher, *Chem. Mater.*, 2009, **21**, 4608.